Entanglement Entropy and Entanglement Growth in Gauge Theory

Naoki Watamura

January 2018

To My Parents

Contents

It often happens in scientific research that when one is looking for one thing, one is led to discover something else that one wasn't expecting.

——— P.A.M. Dirac

Chapter 1

Introduction

Since the quantum theory has been proposed by Heisenberg and Schrödinger in 1925 and 1926, it has become an essential concept in understanding nature. Nowadays, quite a number of quantum phenomena are known and investigated for their theoretical understanding and possible application. Among the characteristic properties that distinguish classical theories from their quantized theories, the *quantum entanglement* receives increasing attention in various fields of physics.

The Einstein-Podolsky-Rosen (EPR) phenomena [1] is one of the most well known example of entanglement, followed by the discussion with its relation to Bell-inequality [2].[1] The entanglement in quantum mechanics is essentially a phenomenon between two systems or particles. However, in order to discuss this concept in field theory, which is the subject of this thesis, we must deal with the entanglement between two regions in space since the state is now field valued.

In order to discuss the amount of entanglement of two regions in space in field theory, we need an appropriate measure. One quantity for this is the *Entanglement Entropy* (EE), and one of its generalization, the so called Rényi entropy [4]. In the field theory, one major problem is the relation between the EE of a black hole

[1] See also [3].

and the Bekenstein-Hawking entropy [5, 6, 7]. In this case, the EE measures the entanglement of two regions, one is inside the black hole behind the event horizon, and the other is its complement.

Kabat compared in his work [8] EE with the one-loop correction from matter fields to the black hole entropy. They agreed for the spin 0 and 1/2, but not for spin 1. For spin 1 field, he found a negative contribution to the entropy, which he called contact term, that can result a negative value of entropy. This was disturbing since, not only the mismatch with the EE, but also contradicting to the fact that entropy is a positive value by its definition.

Even more, it turned out that the EE of gauge fields gives different results depending on their scheme of calculation which caused much controversy [8, 9, 10, 11, 12, 13, 14, 15]. This mismatch of EE was resolved by Donnelly and Wall as the EE of the edge modes living on the boundary [16], that are the classical solutions determined by the electric field normal to the entangling surface.

These problems of EE in gauge theory originate from the fact that we cannot define a gauge invariant tensor decomposition of Hilbert space. In other words, the Gauss law constraint imposes a relation between physical states on the two sides of the boundary [17]. This is crucial since this decomposition is needed to define EE, and as a result the EE depends on the gauge choice.

Therefore, there is no proper definition of EE for gauge fields. Even if there is no gauge independent definition of EE for gauge theory yet, it is important to understand the basic property of entanglement of gauge fields. It is known that if we consider an excited state, we can get such a quantity.

Recently, the Rényi EE of *Locally Excited States* was introduced in [18]. Locally excited state is a state that we obtain by simply acting with a spacetime local operator on the vacuum,

$$|\psi\rangle = \mathcal{O}(x)|0\rangle. \tag{1.1}$$

The time dependence of the Rényi EE of locally excited state has been intensively studied recently, by Nozaki et al [19, 20] and including myself in [21, 22]. In these articles, a quantity was introduced, that is the difference of Rényi EE of the vacuum state and that of a locally excited state, which we call *Rényi EE Growth* in this thesis. It was pointed out, that this Rényi EE growth measures the amount of quantum mechanical degrees of freedom included in an operator [19].

In this thesis, we develop further this idea and we show that the Rényi EE growth can really be decribed as a kind of measure of quantum mechanical degrees of freedom. We also show that under a certain condition the time development of the Rényi EE of this locally excited state is gauge independent. We evaluate several types of excitation and investigate their time development.

This thesis is organized as follows. In chapter 2 we introduce the basic concepts and techniques we use in this thesis. In chapter 3, we describe the Rényi EE growth for scalar fields. Chapter 4, we introduce the *Particle Propagating Model*, and show the relation of Rényi EE growth and its quantum mechanical degrees of freedom. In chapter 5, we discuss the Rényi EE growth for Maxwell fields and its gauge invariance. Chapter 6 is devoted to discussion and conclusion.

Chapter 2

Entanglement Entropy and its Growth

The growth of Entanglement Entropy (EE) for locally excited states of scalar and fermionic fields are studied systematically in the works [18, 19, 20, 23]. Here, we will introduce the definition of the locally excited state and the EE growth. We also introduce the so-called *replica method*, which is the technique we use throughout the QFT calculation in this thesis, both for vacuum state and locally excited state. We explain the case for vacuum in detail since the case for locally excited state is an extension of it.

2.1 Basic Concepts

2.1.1 Quantum Entanglement

Quantum entanglement is a non-local correlation which has no counterpart in classical systems. The concept of quantum entanglement has a simple description in a discrete system.

Consider a two-level system at two points p and q in space. Two-level systems

in quantum mechanics can be represented as up state $|\uparrow\rangle$ and down state $|\downarrow\rangle$. We denote the states of two-level systems in point p and q as $|\uparrow\rangle_p, |\downarrow\rangle_p$ and $|\uparrow\rangle_q, |\downarrow\rangle_q$, respectively. The total Hilbert space for that system is then

$$\mathscr{H} = \mathscr{H}_p \otimes \mathscr{H}_q, \tag{2.1}$$

where $\mathscr{H}_p = \text{Span}\{|\uparrow\rangle_p, |\downarrow\rangle_p\}, \mathscr{H}_q = \text{Span}\{|\uparrow\rangle_q, |\downarrow\rangle_q\}$. Let us consider the following state:

$$|\Psi_1\rangle = \frac{1}{\sqrt{2}} \left(|\uparrow\rangle_p \otimes |\downarrow\rangle_q + |\downarrow\rangle_p \otimes |\uparrow\rangle_q\right). \tag{2.2}$$

In this state, if we know whether the state at p is up or down, then we know immediately the state at point q. On the other hand, if we have a state like

$$|\Psi_2\rangle = \frac{1}{2} \left(|\uparrow\rangle_p + |\downarrow\rangle_p\right) \otimes \left(|\uparrow\rangle_q - |\downarrow\rangle_q\right), \tag{2.3}$$

we can have no information about the point q, by knowing the state at point p. Such a correlated state like (2.2) is called *entangled*, while (2.3) is not.

One quantity to measure the amount of entanglement is the *Entanglement Entropy* (EE). To define EE, let us recall the definition of the density matrix. The density matrices for $|\Psi_1\rangle, |\Psi_2\rangle$ are defined as operators on $\mathscr{H}$:

$$\begin{aligned} \rho^{(1)} &= |\Psi_1\rangle\langle\Psi_1|, \\ \rho^{(2)} &= |\Psi_2\rangle\langle\Psi_2|, \end{aligned} \tag{2.4}$$

respectively.

In general, if the Hilbert space is a tensor product of two subspaces as in equation (2.1), then we can define the reduced density matrix. The reduced density matrix is defined by taking the trace over one subspace, and is an operator on the other subspace. The idea of reduced density matrix was already introduced in 1930 by Paul Dirac [24]. In the present example, the reduced density matrices $\rho_q^{(1)}$ and $\rho_q^{(2)}$,

corresponding to $|\Psi_1\rangle$ and $|\Psi_2\rangle$, respectively, are defined by taking the trace over the Hilbert space $\mathscr{H}_p$

$$\begin{aligned}\rho_q^{(1)} &= \mathrm{tr}_p \rho^{(1)} = \sum_{i=\uparrow,\downarrow} \left({}_p\langle i| \otimes 1_q\right) \rho^{(1)} \left(|i\rangle_p \otimes 1_q\right), \\ \rho_q^{(2)} &= \mathrm{tr}_p \rho^{(2)} = \sum_{i=\uparrow,\downarrow} \left({}_p\langle i| \otimes 1_q\right) \rho^{(2)} \left(|i\rangle_p \otimes 1_q\right),\end{aligned} \tag{2.5}$$

where 1_q is the identity operator acting on $\mathscr{H}_q$, and tr_p is the partial trace over $\mathscr{H}_p$ defined in the right hand side of the equation.

Once one gets the reduced density matrix for a state, one can define the EE as the von Neumann entropy of that reduced density matrix. In the present case, the EE for $\rho_q^{(1)}$ and $\rho_q^{(2)}$ are

$$\begin{aligned}S_{\mathrm{EE}}^{(1)} &= -\mathrm{tr}_q \rho_q^{(1)} \log \rho_q^{(1)} = \log 2, \\ S_{\mathrm{EE}}^{(2)} &= -\mathrm{tr}_q \rho_q^{(2)} \log \rho_q^{(2)} = 0,\end{aligned} \tag{2.6}$$

respectively. We can see in equation (2.6), that the EE for entangled state is non-zero, while that for non-entangled state is zero, and that EE actually reflects the amount of entanglement.

In this thesis, we want to study the property of entanglement in QFT by using this EE and its generalization the Rényi EE. We will give their definitions for QFT in the next section.

2.1.2 Decomposition of Spacetime and Density Matrix

Let $\mathcal{M}$ be a $d+1$-dimensional spacetime with Minkowski signature. The coordinate of a point $p \in \mathcal{M}$ is given by a map x,

$$\begin{aligned} x: \quad & \mathcal{M} \longrightarrow \mathbb{R}^{d+1} \\ & \cup \qquad\quad \cup \\ & p \;\longmapsto x(p) = (x^0(p), x^1(p), \cdots, x^d(p)). \end{aligned} \tag{2.7}$$

Here, we denote the coordinate function as x^μ, and x^0 is the time direction. We use the spacelike signature convention $(-,+,+,\cdots)$.

The submanifold $\mathcal{M}_0$

$$\mathcal{M}_0 = \{p \in \mathcal{M} \mid x^0(p) = 0\}. \tag{2.8}$$

defines a timeslice at $x^0 = 0$.

We divide the timeslice $\mathcal{M}_0$ into two subspaces $\mathcal{A}$ and $\mathcal{B}$. Thus, $\mathcal{A}$ and $\mathcal{B}$ satisfy

$$\begin{aligned} \mathcal{A}, \mathcal{B} &\subset \mathcal{M}_0 \\ \mathcal{B} &= \mathcal{A}^c \end{aligned} \tag{2.9}$$

where $\mathcal{A}^c$ is the complement of $\mathcal{A}$ in $\mathcal{M}_0$. The boundary of $\mathcal{A}$ is denoted as $\partial\mathcal{A}$, that is the intersection of the closure of $\mathcal{A}$ with the closure of its complement:

$$\partial\mathcal{A} := \overline{\mathcal{A}} \cap \overline{\mathcal{A}^c}. \tag{2.10}$$

The boundary $\partial\mathcal{A}$ ($\partial\mathcal{B}$) is called the *entangling surface*, and we denote it as Σ

$$\Sigma = \partial\mathcal{A} = \partial\mathcal{B}. \tag{2.11}$$

Now, we consider a QFT on spacetime $\mathcal{M}$ with the corresponding Hilbert space $\mathscr{H}$. Let the Hilbert space $\mathscr{H}$ spanned by the set of basis $\{|i\rangle\}$

$$\mathscr{H} = \text{Span}\{|i\rangle\}, \tag{2.12}$$

where i is the label for the basis. We assume here that we can decompose this Hilbert space into a tensor product of two subsets $\mathscr{H}_\mathcal{A}$ and $\mathscr{H}_\mathcal{B}$, as

$$\mathscr{H} = \mathscr{H}_\mathcal{A} \otimes \mathscr{H}_\mathcal{B}, \tag{2.13}$$

where $\mathscr{H}_\mathcal{A}$ and $\mathscr{H}_\mathcal{B}$ are the Hilbert spaces associated with the subspaces $\mathcal{A}$ and $\mathcal{B}$, respectively. We denote the basis for $\mathscr{H}_\mathcal{A}$ and $\mathscr{H}_\mathcal{B}$ as $\{|i\rangle_\mathcal{A}\}$ and $\{|i\rangle_\mathcal{B}\}$, respectively, where i is the label of these bases.

The density matrix for an arbitrary pure state $|\psi\rangle \in \mathscr{H}$ is defined as

$$\rho = |\psi\rangle\langle\psi|. \tag{2.14}$$

In general, the density matrix describes also mixed states, which has the form

$$\rho = \sum_i p_i |i\rangle\langle i|, \tag{2.15}$$

where p_i is positive and satisfies $\sum_i p_i = 1$.

If the Hilbert space can be decomposed as described above, the reduced density matrix is then defined as the partial trace of the whole density matrix

$$\rho_{\mathcal{A}} = \mathrm{tr}_{\mathcal{B}}\rho = \sum_i \left(\mathbf{1}_{\mathcal{A}} \otimes {}_{\mathcal{B}}\langle i\,|\right) \rho \ \left(\mathbf{1}_{\mathcal{A}} \otimes |\, i\rangle_{\mathcal{B}}\right), \tag{2.16}$$

where $\mathbf{1}_{\mathcal{A}}$ is the identity operator acting on $\mathscr{H}_{\mathcal{A}}$.

2.1.3 Entanglement Entropy and Rényi Entanglement Entropy

As we explained previously, the EE is defined as the von Neumann entropy of the reduced density matrix

$$S_{\mathcal{A}} = -\mathrm{tr}_{\mathcal{A}}\rho_{\mathcal{A}} \log \rho_{\mathcal{A}}. \tag{2.17}$$

The Rényi EE is defined by the n-th power of the reduced density matrix $\rho_{\mathcal{A}}$, as

$$S_{\mathcal{A}}^{(n)} = \frac{1}{1-n} \log \mathrm{tr}_{\mathcal{A}}\rho_{\mathcal{A}}^n. \tag{2.18}$$

Here, we have assumed that $n > 1$. The Rényi EE has an advantage in practical calculation, namely we can avoid to take the logarithm of a matrix.

In the limit $n \to 1$, the Rényi EE $S_{\mathcal{A}}^{(n)}$ agrees with the definition of EE. This can

be derived easily,

$$\begin{aligned}
\lim_{n\to+1} S_{\mathcal{A}}^{(n)} &= \lim_{n\to+1} -\frac{1}{n-1}\log \mathrm{tr}_{\mathcal{A}}\rho_{\mathcal{A}}^{n} \\
&= \lim_{n\to+1} -\frac{1}{n-1}\left(\log \mathrm{tr}_{\mathcal{A}}\rho_{\mathcal{A}}^{n} - 0\right) \\
&= \lim_{n\to+1} -\frac{1}{n-1}\left(\log \mathrm{tr}_{\mathcal{A}}\rho_{\mathcal{A}}^{n} - \log \mathrm{tr}_{\mathcal{A}}\rho_{\mathcal{A}}\right) \\
&= \lim_{x\to+1} -\partial_x\left(\log \mathrm{tr}_{\mathcal{A}}\rho_{\mathcal{A}}^{x}\right) \\
&= \lim_{x\to+1} -\frac{1}{\mathrm{tr}_{\mathcal{A}}\rho_{\mathcal{A}}^{x}}\mathrm{tr}_{\mathcal{A}}\left(\rho_{\mathcal{A}}^{n}\log\rho_{\mathcal{A}}\right) \\
&= -\mathrm{tr}_{\mathcal{A}}\rho_{\mathcal{A}}\log\rho_{\mathcal{A}}.
\end{aligned} \tag{2.19}$$

where $n \to +1$ or $x \to +1$ means, we take the limit of 1 from the region $n > 1$ and $x > 1$, respectively. Here, we have used the condition $\mathrm{tr}_{\mathcal{A}}\rho_{\mathcal{A}} = 1$. In the replica method, we use this formal relation to get EE.

2.2 The Replica Method

Here we explain the so-called *replica method*. We use the replica method to evaluate the n-th power of the reduced density matrix $\rho_{\mathcal{A}}^{n}$ in QFT. We compute the reduced density matrix $\rho_{\mathcal{A}}$ in the path-integral form, and then formulate the n-th power of it.

We will discuss the path integral representation of the reduced density matrix, first for the vacuum state $\rho_{\mathcal{A}}^{\mathrm{vac}}$ and then for the locally excited state $\rho_{\mathcal{A}}^{\mathrm{ex}}$.

2.2.1 The Case of Vacuum State

The wave functional Ψ on the time slice $x^0 = 0$ is the functional of the field configuration $\phi(x^k)$ on that time slice, where x^k is a space coordinate ($k \in \{1, 2, \cdots d\}$). Considering a vacuum state at past infinity, the wave functional Ψ on the time slice

$x^0 = 0$ is expressed by the path integral as

$$\begin{aligned}\Psi(\phi(x^k)) &= \int_{t=-\infty}^{\psi(x^0=0,x^k)=\phi(x^k)} \mathcal{D}\psi \; e^{i\mathcal{S}[\psi]} \\ &= \int_{x^0=-\infty}^{x^0=0} \mathcal{D}\psi \; e^{i\mathcal{S}[\psi]} \delta\left(\psi(x^0=0,x^k) - \phi(x^k)\right),\end{aligned} \tag{2.20}$$

where $\mathcal{S}[\psi]$ is the action, and $\phi(x^k)$ gives the boundary condition of the path-integral at $x^0 = 0$. We equivalently write $\Psi(\phi(x^k)) = \langle\phi|0\rangle$.

The hermitian conjugate, which is denoted as $\langle 0|\phi\rangle$, can be defined as:

$$\langle 0|\phi\rangle = \Psi^\dagger(\phi(x^k)) = \int_{\psi(x^0=0,x^k)=\phi(x^k)}^{t=\infty} \mathcal{D}\psi \; e^{iS[\psi]}. \tag{2.21}$$

So, if we have two field configurations $\phi_\pm(x^k)$, we are able to write the matrix element of the density matrix as

$$\begin{aligned}\rho(\phi_-(x^k),\phi_+(x^k)) \equiv \langle\phi_-|\rho|\phi_+\rangle &= \mathcal{N}^{-2}\langle\phi_-|0\rangle\langle 0|\phi_+\rangle \\ &= \mathcal{N}^{-2}\Psi(\phi_-(x^k))\Psi^\dagger(\phi_+(x^k)),\end{aligned} \tag{2.22}$$

where the boundary condition of each path integral corresponding to the wave functionals Ψ, $\Psi^\dagger$ is specified by $\phi_\pm(x^k)$, and $\mathcal{N}$ is a normalization constant.

Now, we want to consider the two subregions $\mathcal{A}$ and $\mathcal{B}$. We divide the field configuration $\phi_\pm(x^k)$ according to $\mathcal{A}, \mathcal{B}$.

$$\phi_\pm(x^k(p)) = \begin{cases} \phi_\pm^{\mathcal{A}}(x^k(p)) & p \in \mathcal{A} \\ \phi_\pm^{\mathcal{B}}(x^k(p)) & p \in \mathcal{B} \end{cases} \tag{2.23}$$

where $p \in \mathcal{M}_0$. We can rewrite the above expression of $\langle\phi_-|0\rangle$ in the following form;

$$\langle\phi_-|0\rangle = \begin{cases} \int_{t=-\infty}^{t=0} \mathcal{D}\psi \; e^{iS[\psi]} \delta\left(\psi(t=0,x^k) - \phi_-^{\mathcal{A}}(x^k)\right) & x \in \mathcal{A} \\ \int_{t=-\infty}^{t=0} \mathcal{D}\psi \; e^{iS[\psi]} \delta\left(\psi(t=0,x^k) - \phi_-^{\mathcal{B}}(x^k)\right) & x \in \mathcal{B} \end{cases}, \tag{2.24}$$

where figure (2.1) shows the correspondence between the boundary condition and the region.

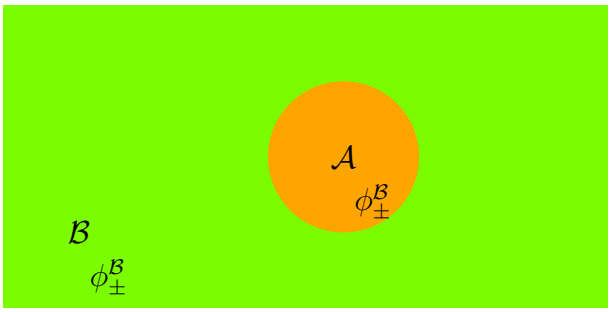

Figure 2.1: Region $\mathcal{A}$,$\mathcal{B}$, and their boundary condition at each region.

As defined in (2.16), to get the reduced density matrix we have to take the partial trace of $\mathscr{H}_{\mathcal{B}}$. This trace can now be defined by using (2.24).

First we introduce a small positive constant $0 < \zeta \ll 1$, and deform the integration region as[1]

$$\langle \phi_-(-\zeta)|0\rangle = \int_{t=-\infty}^{t=-\zeta} \mathcal{D}\psi \; e^{iS[\psi]} \delta\left(\psi(t=-\zeta,x) - \phi_-^{\mathcal{A},\mathcal{B}}(x)\right), \tag{2.25}$$

$$\langle 0|\phi_-(\zeta)\rangle = \int_{t=\zeta}^{t=\infty} \mathcal{D}\psi \; e^{iS[\psi]} \delta\left(\psi(t=\zeta,x) - \phi_-^{\mathcal{A},\mathcal{B}}(x)\right). \tag{2.26}$$

Here we have introduced $\phi_{\pm}^{\mathcal{A},\mathcal{B}}(x)$, which means we choose $\phi_{\pm}^{\mathcal{A}}(x)$ if $x \in \mathcal{A}$ and $\phi_{\pm}^{\mathcal{B}}(x)$ if $x \in \mathcal{B}$. We define the density matrix $\rho(\phi_-, \phi_+, \zeta)$ as

$$\begin{aligned}&\rho(\phi_-,\phi_+,\zeta)\\ &= \frac{1}{Z_1}\int_{t=-\infty}^{t=-\zeta}\int_{t=\zeta}^{t=\infty} \mathcal{D}\psi \; e^{iS[\psi]} \delta\left(\psi(t=-\zeta,x) - \phi_-^{\mathcal{A},\mathcal{B}}(x)\right) \delta\left(\psi(t=\zeta,x) - \phi_+^{\mathcal{A},\mathcal{B}}(x)\right),\end{aligned} \tag{2.27}$$

where in the limit $\zeta \to 0$, this expression matches with the definition of the density matrix in equation (2.22). Z_1 is the normalization constant $Z_1 = \mathcal{N}^2 = \langle 0|0\rangle$.

We are now able to write down the reduced density matrix of the vacuum $\rho_{\mathcal{A}}^{\text{vac}}$ in the path integral form. Taking the trace over $\mathscr{H}_{\mathcal{B}}$ is equal to summing up over the boundary condition $\phi_{\pm}^{\mathcal{B}}$ under the condition $\phi_+^{\mathcal{B}} = \phi_-^{\mathcal{B}}$. Thus by following the

[1] ζ is a small value, which will be taken to zero in the end.

definition (2.16), we get the form

$$\rho_{\mathcal{A}}(\phi_-^{\mathcal{A}}, \phi_+^{\mathcal{A}}, \zeta) = \frac{1}{Z_1} \int \mathcal{D}\phi_-^{\mathcal{B}} \mathcal{D}\phi_+^{\mathcal{B}} \; \rho\left(\phi_-, \phi_+, \zeta\right) \delta(\phi_-^{\mathcal{B}}(x) - \phi_+^{\mathcal{B}}(x)) \tag{2.28}$$

in the limit $\zeta \to 0$, formula (2.28) is the path integral over the spacetime $\mathcal{M}$ with the boundary conditions defined as $\mathcal{A}$; $\phi_-^{\mathcal{A}}(x)$ for $t \to -\zeta$ and $\phi_+^{\mathcal{A}}(x)$ for $t \to +\zeta$.

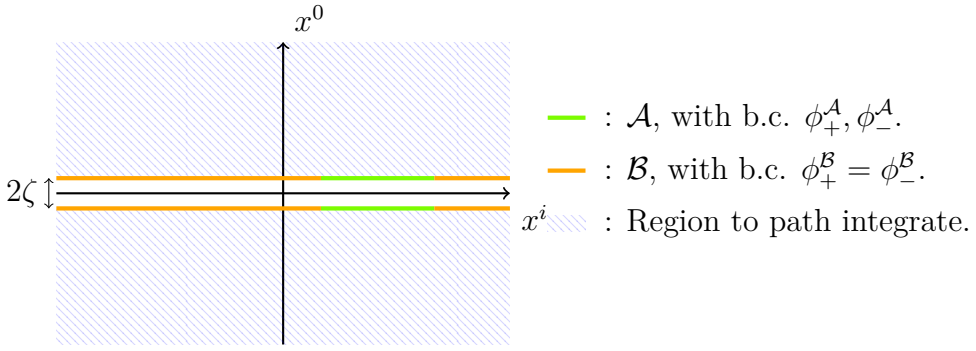

Figure 2.2: The blue lined region is the region to be path integrated. The vertical axis is the x^0 direction, horizontal axis is the space direction.

Figure (2.2) shows schematically the relation of the path integral and boundary condition for the case $\zeta \neq 0$.

In the following, we will move to the Euclidean spacetime. We perform an analytic continuation to imaginary time τ:

$$x^0 = -i\tau. \tag{2.29}$$

Taking powers of this reduced density matrix means, matching the boundary condition of each $\rho_{\mathcal{A}}$. Simply,

$$\begin{aligned}
&\left(\rho_{\mathcal{A}}^2\right)\left(\phi_-^{\mathcal{A},(1)}, \phi_+^{\mathcal{A},(2)}, \zeta\right) \\
&= \int \mathcal{D}\phi_+^{\mathcal{A},(1)} \mathcal{D}\phi_-^{\mathcal{A},(2)} \delta\left(\phi_+^{\mathcal{A},(1)} - \phi_-^{\mathcal{A},(2)}\right) \rho_{\mathcal{A}}\left(\phi_-^{\mathcal{A},(1)}, \phi_+^{\mathcal{A},(1)}, \zeta\right) \rho_{\mathcal{A}}\left(\phi_-^{\mathcal{A},(2)}, \phi_+^{\mathcal{A},(2)}, \zeta\right)
\end{aligned} \tag{2.30}$$

Therefore, the trace of the n-th power of the reduced density matrix $\mathrm{tr}_{\mathcal{A}}\rho_{\mathcal{A}}^n$ is, after taking the limit $\zeta \to 0$,

$$\begin{aligned} \mathrm{tr}_{\mathscr{H}_{\mathcal{A}}}\left(\rho_{\mathcal{A}}^n\right) &= \lim_{\zeta\to 0}\int \mathcal{D}\phi_-^{\mathcal{A},(1)}\mathcal{D}\phi_+^{\mathcal{A},(n)}\delta\left(\phi_-^{\mathcal{A},(1)}-\phi_+^{\mathcal{A},(n)}\right)\left(\rho_{\mathcal{A}}^n\right)\left(\phi_-^{\mathcal{A},(1)},\phi_+^{\mathcal{A},(n)},\zeta\right) \\ &= \left(Z_1\right)^{-n}\int_{\mathcal{M}^{(n)}}\mathcal{D}\psi e^{-S_E[\psi]}, \end{aligned} \tag{2.31}$$

where S_E is the Euclidean action. This path integral runs over the space $\mathcal{M}^{(n)}$, where $\mathcal{M}^{(n)}$ is defined as follows. $\mathcal{M}^{(n)}$ is a manifold which consits of n copies of the spacetime $\mathcal{M}$ connected by a cut at the subregion $\mathcal{A}$ to each other as described in figure 2.3. We define the integral part of the last line in equation (2.31) as Z_n,

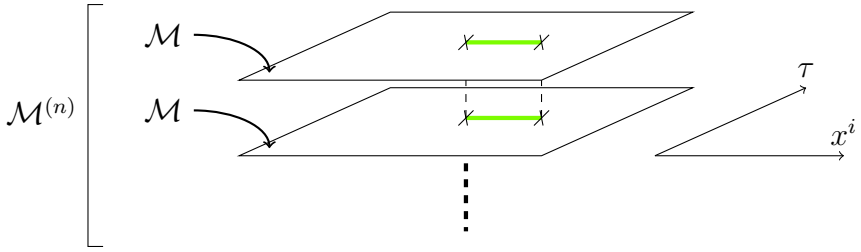

Figure 2.3: Schematic description of $\mathrm{tr}_{\mathcal{A}}\rho_{\mathcal{A}}^n$. Each sheet is isomorphic to $\mathcal{M}$ with a cut in subregion $\mathcal{A}$, which is connected to another $\mathcal{M}$-sheet there. There are n $\mathcal{M}$-sheets, so if one draws a line from any sheet, after crossing the nth cut one returns to the first sheet.

$$Z_n := \int_{\mathcal{M}^{(n)}}\mathcal{D}\psi\ e^{-S_E[\psi]} \tag{2.32}$$

and write (2.31) simply

$$\mathrm{tr}_{\mathcal{A}}\left(\rho_{\mathcal{A}}\right)^n = \frac{Z_n}{Z_1^n}. \tag{2.33}$$

Thus the Rényi EE of this state is

$$\begin{aligned} S_{\mathcal{A}}^{(n)} &= \frac{1}{1-n}\log \mathrm{tr}_{\mathcal{A}}\rho_{\mathcal{A}}^n \\ &= \frac{1}{1-n}\log\frac{Z_n}{Z_1^n}. \end{aligned} \tag{2.34}$$

2.2.2 The Case of Excited State

The discussion for the replica method for locally excited state is parallel to the above discussion of vacuum state, except that we introduce explicitly a regularization parameter ϵ here to avoid the divergence.

We start with a locally excited state $|\psi^{\rm ex}\rangle$ defined in Minkowski spacetime as

$$|\psi^{\rm ex}\rangle = e^{-\epsilon H}\mathcal{O}(t,x)|0\rangle, \tag{2.35}$$

where $\mathcal{O}$ is an operator local in spacetime inserted at (t,x) with $t<0$, and $\epsilon>0$ is a regularization parameter introduced here[2]. The density matrix ρ of this state is

$$\begin{aligned}\rho &= |\psi^{\rm ex}\rangle\langle\psi^{\rm ex}| &(2.36)\\ &= e^{-\epsilon H}\mathcal{O}(t,x)|0\rangle\langle 0|\mathcal{O}^\dagger(t,x)e^{-\epsilon H} &(2.37)\\ &= e^{(it-\epsilon)H}\mathcal{O}(x)|0\rangle\langle 0|\mathcal{O}^\dagger(x)e^{-(it+\epsilon)H}. &(2.38)\end{aligned}$$

Now, we move to Euclidean time. We define $\tau_e = -\epsilon$ and $\tau_l = \epsilon$, and define the density matrix in Euclidean spacetime

$$\begin{aligned}\rho &= e^{\tau_e H}\mathcal{O}(x)|0\rangle\langle 0|\mathcal{O}^\dagger(x)e^{-\tau_l H} &(2.39)\\ &= \mathcal{O}(\tau_e,x)|0\rangle\langle 0|\mathcal{O}^\dagger(\tau_l,x). &(2.40)\end{aligned}$$

We choose τ_e and τ_l so that we recover the density matrix by the analytic continuation $\tau_e = it-\epsilon$ and $\tau_l = it+\epsilon$.

The corresponding wave functional is, in the path-integral form,

$$\begin{aligned}\langle\phi|\psi^{\rm ex}\rangle &= \langle\phi|\mathcal{O}(\tau_e,x)|0\rangle &(2.41)\\ &= \int_{t=-\infty}^{t=0}\mathcal{D}\psi\ \mathcal{O}(\tau_e,x)e^{-S_E[\psi]}\delta\left(\psi(0,x^i)-\phi(x^i)\right). &(2.42)\end{aligned}$$

[2]If $t>0$, the following discussion will be completely the same as in vacuum state, since we are interested in the wave functional at $t=0$.

where S_E is the Euclidean action. The hermitian conjugate is

$$\langle \psi^{\rm ex} \mid \phi \rangle = \langle 0|\mathcal{O}^\dagger(\tau_l, x)|\phi\rangle \tag{2.43}$$

$$= \int_{t=0}^{t=\infty} \mathcal{D}\psi \ \mathcal{O}^\dagger(\tau_l, x) e^{-S_E[\psi]} \delta\left(\psi(0, x^i) - \phi(x^i)\right). \tag{2.44}$$

The reduced density matrix $\rho_{\mathcal{A}}^{\rm ex}$ for this state is

$$\rho_{\mathcal{A}}^{\rm ex}(\phi_0^{\mathcal{A},-}, \phi_0^{\mathcal{A},+}) = \frac{1}{Z_1^{\rm EX}} \int_{\mathcal{M}} \mathcal{D}\psi \ \mathcal{O}^\dagger(\tau_l, x)\mathcal{O}(\tau_e, x) e^{-S_E[\psi]} \delta(\psi(-\zeta, x) - \phi_0^{\mathcal{A},-}(x)) \delta(\psi(\zeta, x) - \phi_0^{\mathcal{A},+}(x)), \tag{2.45}$$

where we have introduced the regulator $Z_1^{\rm EX}$ defined as

$$Z_1^{\rm EX} = \int_{\mathcal{M}} \mathcal{D}\psi \ \mathcal{O}^\dagger(\tau_l, x)\mathcal{O}(\tau_e, x) e^{-S_E[\psi]}. \tag{2.46}$$

In the same way as discussed in the last section, the n-th power of the reduced density matrix becomes

$$\mathrm{tr}_{\mathcal{A}} \left(\rho_{\mathcal{A}}^{\rm ex}\right)^n = \frac{1}{(Z_1^{\rm EX})^n} \int_{\mathcal{M}^{(n)}} \mathcal{D}\psi \ \left(\prod_{k=1}^{n} \mathcal{O}^\dagger(\tau_l, x, k)\mathcal{O}(\tau_e, x, k) \right) e^{-S_E[\psi]}, \tag{2.47}$$

where $\mathcal{M}^{(n)}$ is again the manifold which consists of n connected copies of $\mathcal{M}$, and k denotes the number of the copy on which the operators $\mathcal{O}$ and $\mathcal{O}^\dagger$ are located.

2.3 The Growth of Rényi EE

Here, we give the definition of the Rényi EE growth $\Delta S_{\mathcal{A}}^{(n)}$. The Rényi EE growth $\Delta S_{\mathcal{A}}^{(n)}$ is defined by the difference of the n-th vacuum Rényi EE $S_{\mathcal{A}}^{(n),\rm vac}$ and the n-th Rényi EE of a locally excited state $S_{\mathcal{A}}^{(n),\rm ex}$, i.e.

$$\Delta S_{\mathcal{A}}^{(n)} = S_{\mathcal{A}}^{(n),\rm ex} - S_{\mathcal{A}}^{(n),\rm vac}, \tag{2.48}$$

where $S_{\mathcal{A}}^{(n),\mathrm{ex}}$ is the n-th Rényi EE of locally excited state defined in (2.35). The definitions (2.18), (2.33) and (2.47), lead $\Delta S_{\mathcal{A}}^{(n)}$ to the form

$$\begin{aligned}
\Delta S_{\mathcal{A}}^{(n)} &= -\frac{1}{n-1}\log \mathrm{tr}_{\mathcal{A}}\left(\rho_{\mathcal{A}}^{\mathrm{ex}}\right)^n + \frac{1}{n-1}\log \mathrm{tr}_{\mathcal{A}}\left(\rho_{\mathcal{A}}^{\mathrm{vac}}\right)^n \\
&= -\frac{1}{n-1}\log\left[\frac{\left(\rho_{\mathcal{A}}^{\mathrm{ex}}\right)^n}{\left(\rho_{\mathcal{A}}^{\mathrm{vac}}\right)^n}\right] \\
&= -\frac{1}{n-1}\log\left(\frac{\int_{\mathcal{M}^{(n)}}\mathcal{D}\psi\ \left(\prod_{k=1}^n \mathcal{O}^\dagger(\tau_l,x,k)\mathcal{O}(\tau_e,x,k)\right)e^{-S_E[\psi]}}{\left(Z_1^{\mathrm{EX}}\right)^n}\right)\left(\frac{Z_n}{(Z_1)^n}\right)^{-1} \\
&= -\frac{1}{n-1}\log\left(\frac{\int_{\mathcal{M}^{(n)}}\mathcal{D}\psi\ \left(\prod_{k=1}^n \mathcal{O}^\dagger(\tau_l,x,k)\mathcal{O}(\tau_e,x,k)\right)e^{-S_E[\psi]}}{Z_n}\right) \\
&\qquad\qquad \left(\frac{\int_{\mathcal{M}}\mathcal{D}\psi\ \mathcal{O}^\dagger(\tau_l,x)\mathcal{O}(\tau_e,x)e^{-S_E[\psi]}}{Z_1}\right)^{-n} \\
&= -\frac{1}{n-1}\log\frac{\langle 0|\left(\prod_{k=1}^n \mathcal{O}^\dagger(\tau_l,x,k)\mathcal{O}(\tau_e,x,k)\right)|0\rangle_{\mathcal{M}^{(n)}}}{\left(\langle 0|\mathcal{O}^\dagger(\tau_l,x)\mathcal{O}(\tau_e,x)|0\rangle_{\mathcal{M}}\right)^n}.
\end{aligned} \tag{2.49}$$

In the last line, $\langle 0|\left(\prod_{k=1}^n \mathcal{O}^\dagger(\tau_l,x,k)\mathcal{O}(\tau_e,x,k)\right)|0\rangle_{\mathcal{M}^{(n)}}$ is the $2n$-point function on $\mathcal{M}^{(n)}$, and $\langle 0|\mathcal{O}^\dagger(\tau_l,x)\mathcal{O}(\tau_e,x)|0\rangle_{\mathcal{M}}$ is the 2-point function on $\mathcal{M}$. Therefore, we end up with the expression

$$\Delta S_{\mathcal{A}}^{(n)} = -\frac{1}{n-1}\log\frac{\langle 0|\left(\prod_{k=1}^n \mathcal{O}^\dagger(\tau_l,x,k)\mathcal{O}(\tau_e,x,k)\right)|0\rangle_{\mathcal{M}^{(n)}}}{\left(\langle 0|\mathcal{O}^\dagger(\tau_l,x)\mathcal{O}(\tau_e,x)|0\rangle_{\mathcal{M}}\right)^n}. \tag{2.50}$$

Strictly speaking, the expression (2.48) is defined only at $n \in \{x \in \mathbb{N} \mid x > 1\}$. However, we have seen in (2.19), when we can take the limit $n \to 1$, $\Delta S_{\mathcal{A}}^{(n)}$ becomes the difference of EE.

2.4 Analytic Continuation to Real Time

In this method, the $2n$-point function of $\mathcal{O}$ in $\mathcal{M}^{(n)}$ and the 2-point function of $\mathcal{O}$ in $\mathcal{M}^{(1)}$ give $\Delta S_{\mathcal{A}}^{(n)}$ in Euclidean spacetime. In order to study the dynamics of entanglement in Minkowski spacetime, we perform the analytic continuation to the

real time as in the articles [18, 19, 25, 26, 27, 28, 21]. The analytic contiunation to the real time is performed by

$$\begin{aligned} \tau_e &= it - \epsilon \\ \tau_l &= it + \epsilon \end{aligned} \tag{2.51}$$

where ϵ acts as a smearing parameter which keeps the norm of the locally excited state finite. During the calculation, we keep ϵ finite, but in the end we take the limit $\epsilon \to 0$.

Note that in the analytic continuation in Maxwell theory, the time direction of gauge connection A_μ and derivative $\partial_\mu = \frac{\partial}{\partial x^\mu}$ also change due to covariance. They transform as

$$\begin{aligned} A_\tau &= -iA_t \\ \partial_\tau &= -i\partial_t \end{aligned} \tag{2.52}$$

where A_τ, ∂_τ are the connection and derivative in Euclidean spacetime, and A_t, ∂_t are the connection and derivative in Minkowski spacetime, respectively.

Chapter 3

Rényi EE Growth of Scalar Fields

In this thesis, our goal is to understand the characteristics of Rényi EE growth $\Delta S_{\mathcal{A}}^{(n)}$ in flat spacetime caused by an insertion of a spacetime local operator.

3.1 Space Decomposition

In this chapter, we start by considering the case of free scalar fields. The spacetime $\mathcal{M}$ here is flat $d+1$-dimension with Minkovski signature:

$$\mathcal{M} = \mathbb{R}^{d+1}, \tag{3.1}$$

and for the metric, we use the spacelike signature convention:

$$g_{\mu\nu} = \eta_{\mu\nu} = \begin{cases} -1 & \mu = \nu = 0 \\ \delta_{\mu\nu} & \text{else} \end{cases}. \tag{3.2}$$

The coordinate of a point $p \in \mathcal{M}$ is given by a map x,

$$\begin{aligned} x: \quad & \mathcal{M} \longrightarrow \mathbb{R}^{d+1} \\ & \cup \qquad \cup \\ & p \ \longmapsto x(p) = (x^0(p), x^1(p), \cdots, x^d(p)), \end{aligned} \tag{3.3}$$

and the submanifold $\mathcal{M}_0$ is chosen as the time slice of $x^0 = 0$:

$$\mathcal{M}_0 = \{p \in \mathcal{M} \mid x^0(p) = 0\}. \tag{3.4}$$

We divide $\mathcal{M}_0$ into two subregions $\mathcal{A}$ and $\mathcal{B}$ as

$$\begin{aligned} \mathcal{A} &= \{p \in \mathcal{M}_0 \mid x^1(p) \geq 0\}, \\ \mathcal{B} &= \{p \in \mathcal{M}_0 \mid x^1(p) < 0\}. \end{aligned} \tag{3.5}$$

Figure (3.1) shows how we have divided the subspace $\mathcal{M}_0$. Since the entangling

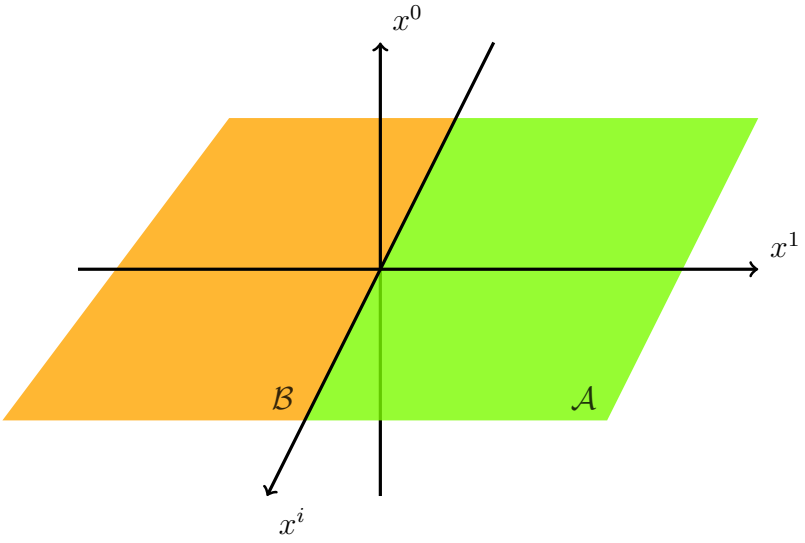

Figure 3.1: The way to choose the regions $\mathcal{A}$ and $\mathcal{B}$ on $\mathcal{M}_0$. x^i describes any direction other than x^0 or x^1, thus $i \in \{2, 3, \cdots n\}$.

surface Σ is given by $x^1 = 0$, the system has remaining symmetries. One is a translational symmetry along the surface Σ, and a rotational symmetry $\mathrm{SO}(d-1)$ with rotation axes orthogonal to the entangling surface Σ.

The QFT we are considering here is the free massless scalar field theory, which has the simple Lagrangian

$$\mathscr{L} = -\frac{1}{2}\partial_\mu \phi^\dagger \partial^\mu \phi. \tag{3.6}$$

We consider the insertion of the spacetime local operator to generate the excited state $|\psi^{\text{ex}}\rangle$ at the point $x^0 = -t, x^1 = -\ell$ and $x^i = 0$ for $i > 1$, as shown in Figure 3.2. The locally excited state we consider here is therefore described as

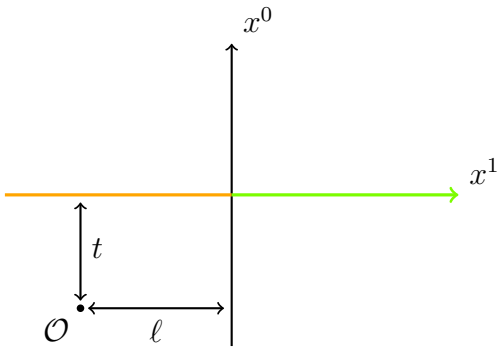

Figure 3.2: Insertion point of the spacetime local operator in Minkovski spacetime.

$$|\psi^{\text{ex}}\rangle = \mathcal{N}\mathcal{O}(-t, -\ell)|0\rangle \tag{3.7}$$

where $\mathcal{N}$ is a normalization constant. The coordinate x^i for $i \geqq 2$ is suppressed, since we can set them to zero without loss of generality due to the translational symmetry.

As mentioned in the previous section, we take a Wick rotation to Euclidean time. For convenience, we will take the polar coordinates for the x^0 and x^1 direction, (r, θ). Figure 3.3 shows the insertion points of the local operators in Euclidean spacetime using polar coordinates (r, θ).

3.2 Rényi EE Growth $\Delta S_{\mathcal{A}}^{(n)}$ for Scalar Fields

3.2.1 Single Operator Insertion

We discuss here the insertion of one scalar field ϕ, i.e. we choose the local operator to be $\mathcal{O} = \phi$. As we explained in the previous section (see equation (2.50)), the

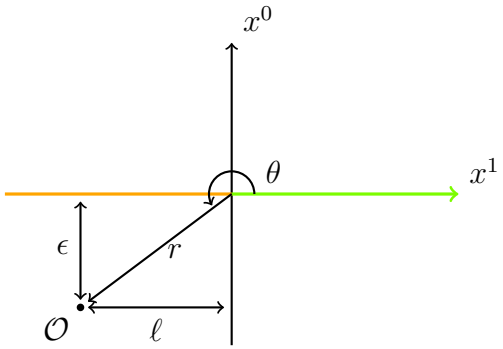

Figure 3.3: Insertion point of the operator in Euclidean spacetime.

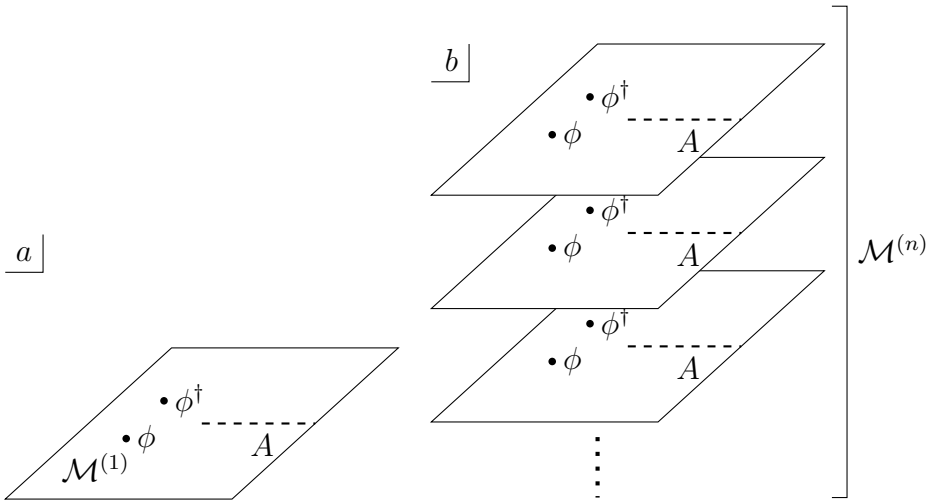

Figure 3.4: The sketch of inserted operators on a) $\mathcal{M}^{(1)}$ and b) $\mathcal{M}^{(n)}$.

corresponding Rényi EE growth $\Delta S_{\mathcal{A}}^{(n)}$ is

$$\Delta S_{\mathcal{A}}^{(n)} = \frac{1}{1-n} \log \frac{\langle 0| \left(\prod_{k=1}^{n} \phi^\dagger(\tau_l, x, k) \phi(\tau_e, x, k) \right) |0\rangle_{\mathcal{M}^{(n)}}}{\left(\langle 0|\phi^\dagger(\tau_l, x)\phi(\tau_e, x)|0\rangle_{\mathcal{M}^{(1)}} \right)^n}. \tag{3.8}$$

Thus, we need the $2n$-point function on $\mathcal{M}^{(n)}$, and the 2-point function on $\mathcal{M}^{(1)}$. The insertion points of the scalar field on the manifold $\mathcal{M}^{(n)}$ is shown in figure 3.4. The 2-point function on $\mathcal{M}^{(n)}$ is known [18] as

$$G_d^{(n)}(r,r',\theta,\theta',x,x')$$
$$= \frac{\Gamma\left(\frac{d-1}{2}\right)}{4n\pi(2\sqrt{\pi})^{d-1}} \frac{1}{2\pi i} \sum_{l=0}^{\infty} d_l \int_{\infty-i\pi}^{\infty+i\pi} dt \frac{4^{\frac{d-1}{2}} e^{-\frac{l}{n}t} cos\left(\frac{l(\theta-\theta')}{n}\right)}{\left((x-x')^2 + r^2 + r'^2 - 2rr'\cosh t\right)^{\frac{d-1}{2}}} \tag{3.9}$$

where $d_l = 1$ for $l = 0$ and $d_l = 2$ for $l \geqq 1$, (r, θ, x) and (r', θ', x') are the coordinates of the scalar operators on $\mathcal{M}^{(n)}$ in polar coordinates.

In the following, we give an explicit example for the case $d = 3$, where we can perform this integral. The 2-point function is obtained as

$$G_3^{(n)}(r,r',\theta,\theta') = \frac{1}{4n\pi^2 rr'(a-a^{-1})} \frac{a^{\frac{1}{n}} - a^{-\frac{1}{n}}}{a^{\frac{1}{n}} + a^{-\frac{1}{n}} - 2\cos\left(\frac{\theta-\theta'}{n}\right)} \tag{3.10}$$

where a is given by

$$\frac{a}{1+a^2} = \frac{rr'}{(x-x')^2 + r^2 + r'^2}. \tag{3.11}$$

In this way, we have determined the propagator.

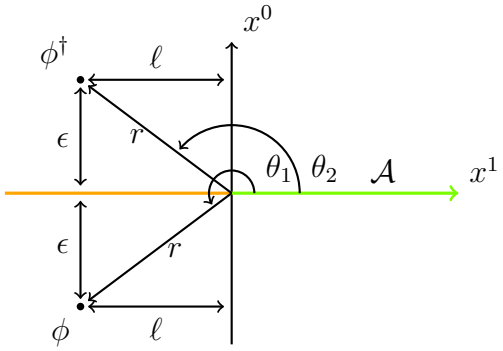

Figure 3.5: Insertion points of the operators in Euclidean coordinates.

In order to understand how to determine the $2n$-point function, we need to explain some more details. Figure 3.5 shows the insertion points of scalar operators on each copy $\mathcal{M}$ of $\mathcal{M}^{(n)}$ in figure 3.4 (b). By the definition of the replica method, the insertion points of the scalar field ϕ and its hermitian conjugate $\phi^\dagger$ are symmetric with respect to the x^1 axis. In terms of polar coordinates, this means $\theta_1 + \theta_2 = 2\pi$.

The angle dependence of the Green's function (3.10) appears only in the form of a difference, which is $\theta - \theta'$. The angle difference of scalar operators ϕ and $\phi^\dagger$ is $\theta_1 - \theta_2 + 2\pi k$, where k is an integer. If $k = 0$, this is the relative angle for operators on the same sheet, and if $k \neq 0$, this is the relative angle for operators on different sheets.

Therefore, the 2-point function relevant now can be simplified from equation (3.10), and has the form

$$G_3^{(n)}(r, r, \theta_1 - \theta_2 + 2\pi k) = \frac{1}{4n\pi^2 r^2 (a - a^{-1})} \frac{a^{\frac{1}{n}} - a^{-\frac{1}{n}}}{a^{\frac{1}{n}} + a^{-\frac{1}{n}} - 2\cos\left(\frac{\theta_1 - \theta_2 + 2\pi k}{n}\right)}, \quad (3.12)$$

where k is an integer between 0 and $n - 1$.

After the analytic continuation to the real time, the leading term in the ϵ expansion of the 2-point functions depends on the two parameters t and ℓ, which play an important role in the time evolution later. For the region $t \geqq \ell$, the 2-point function ϵ dependence is

$$G_3^{(1)}(r, r, \theta_1 - \theta_2) = \frac{1}{16\pi^2\epsilon^2} + O(\epsilon^{-1}) \quad (3.13)$$

$$G_3^{(n)}(r, r, \theta_1 - \theta_2 + 2\pi k) = \begin{cases} \frac{t + (1-2k)\ell}{32\pi^2 t\epsilon^2} + O(\epsilon^{-1}) & k = 0, 1 \\ O(\epsilon^{-1}) & k = 2, \cdots, n \end{cases}. \quad (3.14)$$

where $n \geqq 2$. For the region $t < \ell$, the 2-point funcion ϵ dependence is

$$G_3^{(n)}(r, r, \theta_1 - \theta_2 + 2\pi k) = \begin{cases} \frac{1}{16\pi^2\epsilon^2} + O(\epsilon^{-1}) & k = 0, 1 \\ O(\epsilon^0) & k = 2, \cdots, n \end{cases} \quad (3.15)$$

where $n \geqq 1$.

Let us recall the Rényi EE growth $\Delta S_{\mathcal{A}}^{(n)}$ given in (3.8). The numerator of the Rényi EE growth is given by the $2n$-point function on $\mathcal{M}^{(n)}$, which can be evaluated by the Wick contraction rule using the above 2-point function (3.14). On the other hand, the denominator is the n-th power of the 2-point function on $\mathcal{M}^1$, and thus

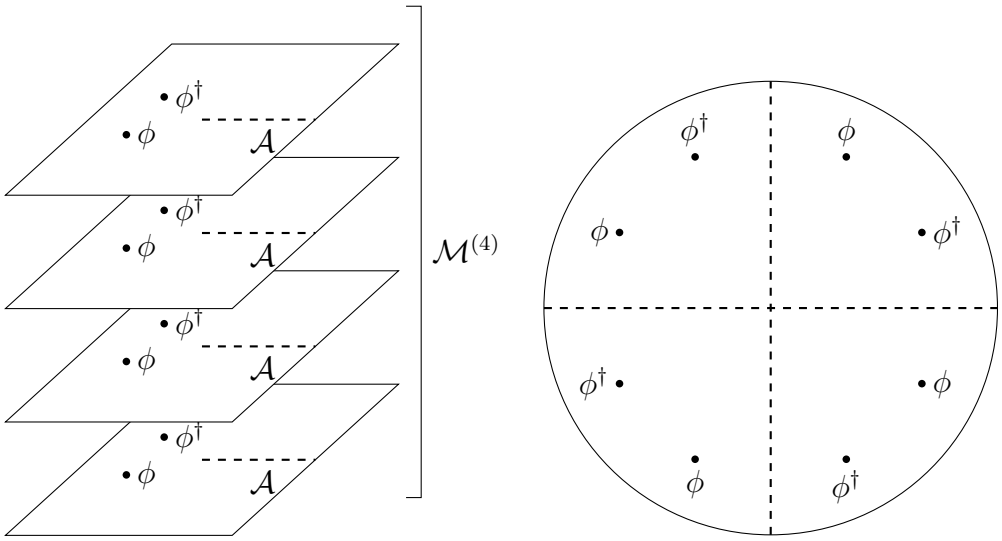

Figure 3.6: The schematic sketch of $\mathcal{M}^{(4)}$. The dashed lines represent the cuts on manifold $\mathcal{M}^{(n)}$, which correspond to the subregion $\mathcal{A}$.

the leading ϵ dependence of the denominator is ϵ^{-2n}. As a result, only the $2n$-point function constructed by propagators of $k = 0, 1$ contribute to the Rényi EE growth after taking the limit $\epsilon \to 0$. There are two types of contaction, one is only using the propagator with $k = 0$, and the other is only using the propagator with $k = 1$. This can be understood by the following diagramatic method.

Let us represent the manifold $\mathcal{M}^{(n)}$ as one disk. Note that we are not performing any coordinate transformation here, but just rewriting the topological structure of the manifold $\mathcal{M}^{(n)}$ with inserted operators and cuts. Figure 3.6 shows the case for $n = 4$. The two diagrams corresponding to the case $k = 0$ and $k = 1$ are obtained by contracting two neighboring operators ϕ and $\phi^\dagger$.

Figure 3.7 shows the diagrams which contribute to 4th Rényi EE growth $\Delta S_{\mathcal{A}}^{(4)}$. In the diagram, the line connecting two insertion points represents the contraction of the corresponding two operators. The propagator $k = 0$ corresponds to the line which does not cross the cuts, and the propagator $k = 1$ corresponds to the line

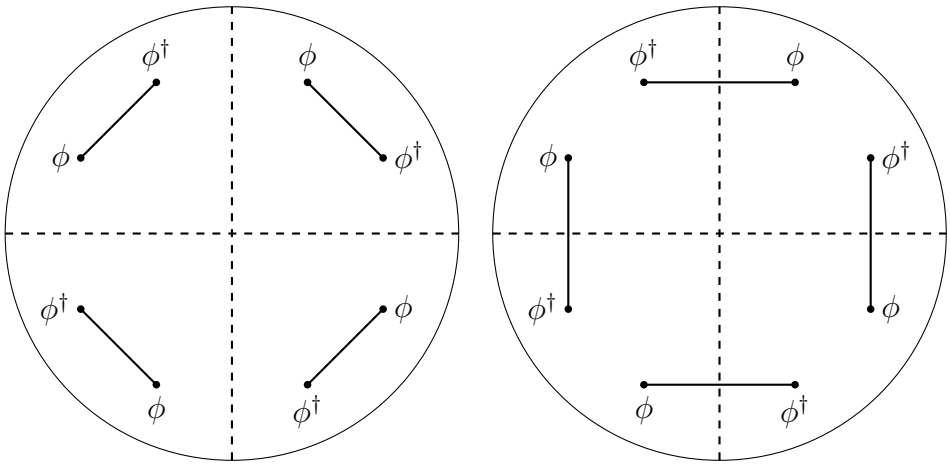

Figure 3.7: Diagrams which contributes to $\Delta S_{\mathcal{A}}^{(4)}$.

which crosses the cut. Explicitly, for $n = 4$ we obtain,

$$\frac{\langle 0|\phi^\dagger\phi\phi^\dagger\phi\phi^\dagger\phi\phi^\dagger\phi|0\rangle}{\left(\langle 0|\phi^\dagger\phi|0\rangle\right)^4} = \left(\frac{G_3^{(4)}(\theta_1-\theta_2)}{G_3^{(1)}(\theta_1-\theta_2)}\right)^4 + \left(\frac{G_3^{(4)}(\theta_2-\theta_1+2\pi)}{G_3^{(1)}(\theta_1-\theta_2)}\right)^4 \tag{3.16}$$

where the propagators are given in (3.13) and (3.14) with the arguments r suppressed. We can show that in the limit $\epsilon \to 0$ the terms $\frac{G^{(n)}(\theta_1-\theta_2)}{G^{(1)}(\theta_1-\theta_2)}$ and $\frac{G^{(n)}(\theta_2-\theta_1+2\pi)}{G^{(1)}(\theta_1-\theta_2)}$ are exactly the same for $n = 2, 3, 4$. Thus, we assume that these two functions are the same for arbitrary n. Then we get the Rényi EE growth $\Delta S_{\mathcal{A}}^{(n)}$ for $t \geqq \ell$,

$$\begin{aligned}\Delta S_{\mathcal{A}}^{(n)} &= \frac{1}{1-n}\log\left(\left(\frac{G_3^{(2)}(\theta_1-\theta_2)}{G_3^{(1)}(\theta_1-\theta_2)}\right)^n + \left(\frac{G_3^{(2)}(\theta_2-\theta_1+2\pi)}{G_3^{(1)}(\theta_1-\theta_2)}\right)^n\right) \\ &= \frac{1}{1-n}\log\left(\left(\frac{t+\ell}{2t}\right)^n + \left(\frac{t-\ell}{2t}\right)^n\right)\end{aligned} \tag{3.17}$$

For $n = 2$ case,

$$\Delta S_{\mathcal{A}}^{(2)} = -\log\left(\left(\frac{t+\ell}{2t}\right)^2 + \left(\frac{t-\ell}{2t}\right)^2\right) \tag{3.18}$$

is the result for $t \geqq \ell$. Figure 3.8 is the plot of Rényi EE growth $\Delta S_{\mathcal{A}}^{(2)}$. We can see that the Rényi EE growth is zero until $t = \ell$, which means that until this point the Rényi EE is equivalent with the vacuum Rényi EE, and then it starts growing.

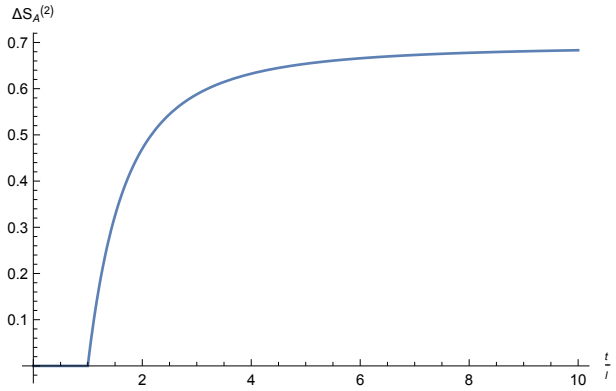

Figure 3.8: The growth of 2nd Rényi EE. The vertical axis is $\Delta S_{\mathcal{A}}^{(2)}$, and the horizontal axis is t/ℓ.

This behaviour is consistent with causality, which we discuss in detail in the next chapter.

In the late time limit $t \to \infty$, the Rényi EE growth is

$$\Delta S_{\mathcal{A}}^{(n)} = \frac{1}{1-n} \log 2^{1-n} = \log 2, \tag{3.19}$$

for arbitrary n.

3.2.2 Composite Operator Insertion

We give an example for the case of inserting a composite operator $\phi^2(-t, -\ell)$. We use the same diagramatic description as figure 3.7. There are now three types of diagrams that contribute to the Rényi EE growth $\Delta S_{\mathcal{A}}^{(n)}$, which are shown in figure 3.9. We have one more diagram than in the previous case, since we have the square of scalar field at each point. The Rényi EE growth for $t > \ell$ has the form:

$$\Delta S_{\mathcal{A}}^{(n)} = \frac{1}{1-n} \log \left[\left(\frac{t+\ell}{2t} \right)^{2n} + \left(\frac{t-\ell}{2t} \right)^{2n} + 2^n \left(\frac{t+\ell}{2t} \right)^{n} \left(\frac{t-\ell}{2t} \right)^{n} \right]. \tag{3.20}$$

where for $t \leqq \ell$ the Rényi EE growth is zero. Figure 3.10 is the plot of 2nd Rényi EE growth. The late time value is

$$\lim_{t\to\infty} \Delta S_{\mathcal{A}}^{(n)} = \frac{1}{1-n} \log \left[2^{-2n+1} + 2^{-n} \right]. \tag{3.21}$$

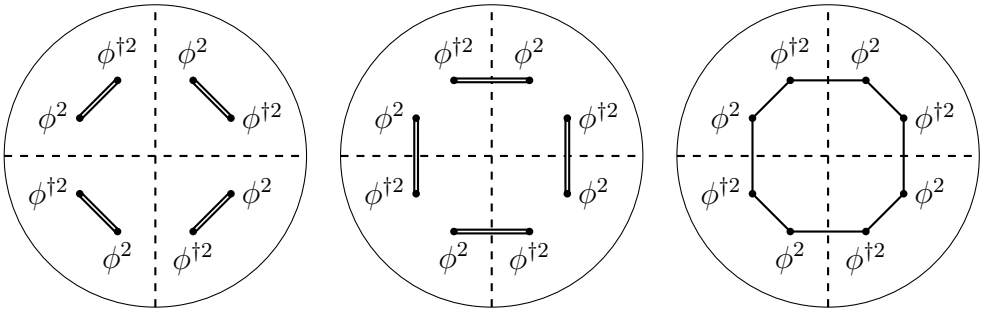

Figure 3.9: Diagrams which contributes to $\Delta S_{\mathcal{A}}^{(4)}$.

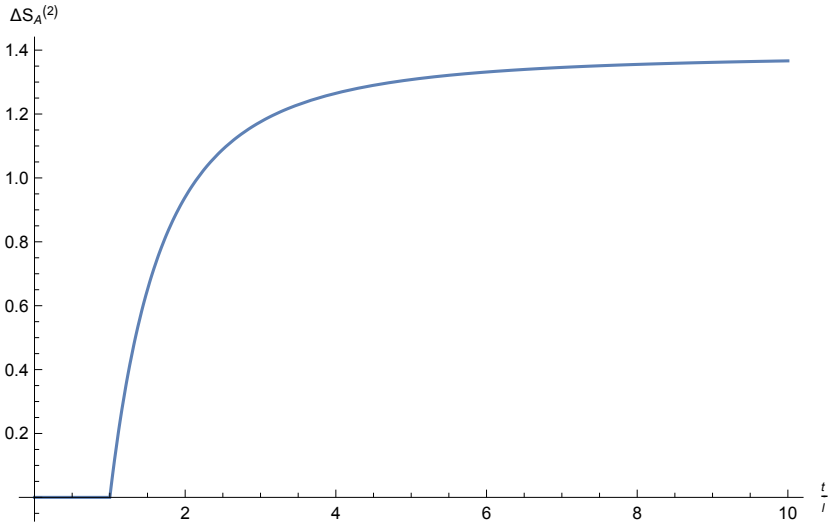

Figure 3.10: The Rényi EE growth $\Delta S_{\mathcal{A}}^{(2)}$ for ϕ^2 insertion. The horizontal axis is time $\frac{t}{\ell}$, the vertical axis is Rényi EE growth $\Delta S_{\mathcal{A}}^{(2)}$.

In the limit $n \to 1$, this becomes $\frac{3}{2}\log 2$, which is the three half of the value of that in the single operator insertion case.

Chapter 4

Quasi-Particle Description of Scalar Fields

In this section, we study the Rényi EE growth $\Delta S_{\mathcal{A}}^{(n)}$ for locally excited states in $d+1$ dimensional spacetime with odd d, $d \geqq 3$. The *late time algebra* is defined, that gives the Rényi EE growth $\Delta S_{\mathcal{A}}^{(n)}$ of half space in the late time limit $t \to \infty$. The Rényi EE growth $\Delta S_{\mathcal{A}}^{(n)}$ at late time has been studied in refs. [18, 19, 26, 25, 27, 28, 21]. In 4 dimensional spacetime, the behaviour of EE of half space can be described by a model with a quasi-particle propagating spherically. An interesting correspondence between an analytic-continued propagator and the probability of a propagating quasi-particle is found.

We will first describe the late time algebra, which describes the late time behaviour of the Rényi EE growth $\Delta S_{\mathcal{A}}^{(n)}$ in terms of the quasi particle picture. After that, the particle propagating model is explained as an extension of the quasi-particle picture.

4.1 Physics of Entanglement Growth

As in the example of the scalar field given in the previous section, the growth of Rényi EE of half space reaches a finite value in every case. This behaviour can be understood physically in the following way, schematically shown in figure 4.1:

By the insertion of a spacetime local operator $\phi(-t, -\ell)$, the operator starts to influence the spacetime entanglement structure from that time on. Since we are inserting a massless scalar field, the effect caused by this operator travels at the speed of light c. For simplicity, we set the speed of light to $c = 1$. Since the distance between the inserted operator ϕ and the entangling surface Σ is ℓ, for the time $t \leqq \ell$, the operator changes only the structure of the region in the subregion $\mathcal{B}$, and thus there is no change of Rényi EE. After time $t = \ell$, the effect of the operator reaches the region $\mathcal{A}$, thus the Rényi EE between $\mathcal{A}$ and $\mathcal{B}$ starts to increase.

At the time $t = \infty$, the effect of insertion is now spread all over the space, and thus each subregion $\mathcal{A}$ and $\mathcal{B}$ divides the effect exactly into half. At this stage the entanglement reaches its maximum, and so does the Rényi EE.

4.2 Late Time Value and Late Time Algebra

We now introuce the *Late Time Algebra* (LTA). LTA is an algebra that gives a quasi-particle description to the Rényi EE growth $\Delta S_{\mathcal{A}}^{(n)}$ in the late time limit $t \to \infty$. The quasi-particle description for scalar, fermions and Maxwell fields was already found in [18, 20, 21]. However, they were given in a somehow ad hoc manner. Here, we introduce a systematical way to determine the LTA.

LTA is an algebra that consists of operators and their commutation relations. We define two operators and their hermite conjugate for the scalar case as follows,

$$\hat{\phi}^{\mathrm{L}}, \hat{\phi}^{\mathrm{L}\dagger}, \hat{\phi}^{\mathrm{R}}, \hat{\phi}^{\mathrm{R}\dagger}, \tag{4.1}$$

where L and R stands for Left and Right mover, respectively. This is in analogy with QFT:

Recall the momentum description of a scalar operator $\phi(x)$. We can separate the scalar operator $\phi(x)$ with respect to the sign of k_1, the momentum along the x^1 axis,

$$\begin{aligned}\phi(x) &= \int \frac{d^d k}{(2\pi)^d 2k^0} \left(\tilde{\phi}\left(k_i\right) e^{ik_\mu x^\mu} + \tilde{\phi}^\dagger(k_i) e^{-ik_\mu x^\mu}\right) \\ &= \int \frac{d^{d-1}k}{(2\pi)^{d-1}} \left[\int_0^\infty \frac{dk^1}{(2\pi)\,2k^0} \left(\tilde{\phi}\left(k_i\right) e^{ik_\mu x^\mu} + \tilde{\phi}^\dagger(k_i) e^{-ik_\mu x^\mu}\right)\right. \\ &\quad \left. + \int_{-\infty}^0 \frac{dk^1}{(2\pi)\,2k^0} \left(\tilde{\phi}\left(k_i\right) e^{ik_\mu x^\mu} + \tilde{\phi}^\dagger(k_i) e^{-ik_\mu x^\mu}\right)\right]. \end{aligned} \tag{4.2}$$

Then, we define the left moving part $\phi^{\mathrm{L}}(x), \phi^{\mathrm{L},\dagger}(x)$ and right moving part $\phi^{\mathrm{R}}(x), \phi^{\mathrm{R},\dagger}(x)$ as

$$\begin{aligned}\phi^{\mathrm{R}}(x) &= \int_0^\infty \frac{dk^1}{2\pi} \int \frac{d^{d-1}k}{(2\pi)^{d-1}2k^0} \tilde{\phi}\left(k_\mu\right) e^{ik_\mu x^\mu}, \\ \phi^{\mathrm{R}\dagger}(x) &= \int_0^\infty \frac{dk^1}{2\pi} \int \frac{d^{d-1}k}{(2\pi)^{d-1}2k^0} \tilde{\phi}^\dagger\left(k_\mu\right) e^{-ik_\mu x^\mu}, \\ \phi^{\mathrm{L}}(x) &= \int_{-\infty}^0 \frac{dk^1}{2\pi} \int \frac{d^{d-1}k}{(2\pi)^{d-1}2k^0} \tilde{\phi}\left(k_\mu\right) e^{ik_\mu x^\mu}, \\ \phi^{\mathrm{L}\dagger}(x) &= \int_{-\infty}^0 \frac{dk^1}{2\pi} \int \frac{d^{d-1}k}{(2\pi)^{d-1}2k^0} \tilde{\phi}^\dagger\left(k_\mu\right) e^{-ik_\mu x^\mu}, \end{aligned} \tag{4.3}$$

where $k^\mu k_\mu = 0$ and $k^0 > 0$. In this way, we can decompose the scalar operator ϕ into

$$\phi(x) = \phi^{\mathrm{L}}(x) + \phi^{\mathrm{L}\dagger}(x) + \phi^{\mathrm{R}}(x) + \phi^{\mathrm{R}\dagger}(x). \tag{4.4}$$

We expect the physics in the late time $t \to \infty$ can be expressed by the corresponding operators $\hat{\phi}^{\mathrm{L}}, \hat{\phi}^{\mathrm{L}\dagger}, \hat{\phi}^{\mathrm{R}}, \hat{\phi}^{\mathrm{R}\dagger}$, where $\hat{\phi}$ is defined by their linear combination as

$$\hat{\phi} = \hat{\phi}^{\mathrm{L}} + \hat{\phi}^{\mathrm{R}} + \hat{\phi}^{\mathrm{L}\dagger} + \hat{\phi}^{\mathrm{R}\dagger}. \tag{4.5}$$

Their commutation relations are proposed as

$$\begin{aligned}\left[\hat{\phi}^{\mathrm{L}}, \hat{\phi}^{\mathrm{L}\dagger}\right] &= C \\ \left[\hat{\phi}^{\mathrm{R}}, \hat{\phi}^{\mathrm{R}\dagger}\right] &= C\end{aligned} \tag{4.6}$$

where C is a constant, and the other combinations are zero.

The Hilbert space on which these operators act is defined as the Fock state of the operators $\hat{\phi}^{\mathrm{L}\dagger}, \hat{\phi}^{\mathrm{R}\dagger}$. We call the Hilbert spaces for each $\hat{\phi}^{\mathrm{L}}$ and $\hat{\phi}^{\mathrm{R}}$ as $\mathscr{H}_{\mathrm{L}}$ and $\mathscr{H}_{\mathrm{R}}$, respectively, and define them as follows,

$$\begin{aligned}\mathscr{H}_{\mathrm{L}} &= \mathrm{Span}\{|0\rangle_{\mathrm{L}}, \hat{\phi}^{\mathrm{L}\dagger}|0\rangle_{\mathrm{L}}, \cdots\}, \\ \mathscr{H}_{\mathrm{R}} &= \mathrm{Span}\{|0\rangle_{\mathrm{R}}, \hat{\phi}^{\mathrm{R}\dagger}|0\rangle_{\mathrm{R}}, \cdots\},\end{aligned} \tag{4.7}$$

where the vacuum states $|0\rangle_{\mathrm{L}}$ and $|0\rangle_{\mathrm{R}}$ satisfy

$$\begin{aligned}\hat{\phi}^{\mathrm{L}}|0\rangle_{\mathrm{L}} &= 0, \\ \hat{\phi}^{\mathrm{R}}|0\rangle_{\mathrm{R}} &= 0.\end{aligned} \tag{4.8}$$

The total Hilbert space is then their tensor product $\mathscr{H}_{\mathrm{L}} \otimes \mathscr{H}_{\mathrm{R}}$, and the normalized n-particle states are defined as follows,

$$\begin{aligned}|n\rangle_{\mathrm{L}} &= \frac{1}{\sqrt{n!C^n}} \left(\hat{\phi}^{\mathrm{L}\dagger}\right)^n |0\rangle_{\mathrm{L}}, \\ |n\rangle_{\mathrm{R}} &= \frac{1}{\sqrt{n!C^n}} \left(\hat{\phi}^{\mathrm{R}\dagger}\right)^n |0\rangle_{\mathrm{R}}.\end{aligned} \tag{4.9}$$

To calculate the late time value of Rényi EE growth of the locally excited state which we have determined in the previous section, we have to choose a corresponding state in LTA. We call this state in $\mathscr{H}_{\mathrm{L}} \otimes \mathscr{H}_{\mathrm{R}}$ as the "effective state" $|\psi^{\mathrm{eff}}\rangle$:

As is expected, as far as the insertion point is in a finite region near the entangling surface Σ, the late time value does not depend on the location of insertion, but only on the number of inserted operators. Thus, we obtain the "effective state" by acting with the same number of the operator $\hat{\phi}$ as one has inserted at the point $(-t, -l)$.

For example, if we choose as locally excited state (2.35),

$$|\psi^{\mathrm{ex}}\rangle = \phi(-t, -\ell)|0\rangle, \tag{4.10}$$

the corresponding "effective state" is obtained by acting with the same number of operator $\hat{\phi}$ in LTA (Note that we take $C = 1$ in the following for simplicity.)

$$\begin{aligned} |\psi^{\text{eff}}\rangle &= \frac{1}{\sqrt{2}} : \hat{\phi} : |0\rangle_{\text{L}} \otimes |0\rangle_{\text{R}} \\ &= \frac{1}{\sqrt{2}} \left(|1\rangle_{\text{L}} \otimes |0\rangle_{\text{R}} + |0\rangle_{\text{L}} \otimes |1\rangle_{\text{R}} \right). \end{aligned} \tag{4.11}$$

where the constant $2^{-\frac{1}{2}}$ is for normalization. The double dot means normal ordering, which is not necessary in this case, but we need it in the case of multiple operator insertion. We can define the *effective density matrix* ρ^{eff} for the effective state $|\psi^{\text{eff}}\rangle$ as

$$\rho^{\text{eff}} = \mathcal{N} |\psi^{\text{eff}}\rangle\langle\psi^{\text{eff}}| \tag{4.12}$$

where $\mathcal{N}$ is a normalization constant.

Since the total Hilbert space of LTA is decomposed as $\mathscr{H}_{\text{L}} \otimes \mathscr{H}_{\text{R}}$, we can define the effective reduced density matrix $\rho_{\text{R}}^{\text{eff}}$ by tracing over the Hilbert space $\mathscr{H}_{\text{L}}$,

$$\rho_{\text{R}}^{\text{eff}} = \text{tr}_{\text{L}} \left(\rho^{\text{eff}} \right). \tag{4.13}$$

Therefore, the Rényi EE of the effective reduced density matrix $\rho_{\text{R}}^{\text{eff}}$ is given by

$$S_{\text{R}}^{(n),\text{LTA}} = \frac{1}{1-n} \text{tr}_{\text{R}} \left[(\rho_{\text{R}}^{\text{eff}})^n \right]. \tag{4.14}$$

We can easily see that this Reńyi EE of LTA, $S_{\text{R}}^{(n),\text{LTA}}$, coincides with the late time value of Rényi EE growth in QFT obtained in section 3.2:

$$S_{\text{R}}^{(n),\text{LTA}} = \lim_{t \to \infty} \Delta S_{\mathcal{A}}^{(n)}. \tag{4.15}$$

4.3 Finite Time Algebra

The LTA introduced in the previous section, gives the late time entanglement structure. We found that this algebra can be extended to the algebra on each time slice

after the insertion. The extension is to define the commutation relation at each time slice between $0 \leqq t < \infty$.

However, we should be careful when we consider a quantum mechanical model with time dependent commutation relation, since such a theory does not have a unitary time development in general.

The algebra we introduce in the following should be considered to be defined on each time slice. We propose the commutation relation,

$$\begin{aligned}\left[\hat{\phi}^{\mathrm{L}}, \hat{\phi}^{\mathrm{L}\dagger}\right] &= \lim_{\epsilon\to 0} 2\frac{G^{(n)}(\theta_1-\theta_2)}{G^{(1)}(\theta_1-\theta_2)} \equiv f_{\mathrm{L}}(t), \\ \left[\hat{\phi}^{\mathrm{R}}, \hat{\phi}^{\mathrm{R}\dagger}\right] &= \lim_{\epsilon\to 0} 2\frac{G^{(n)}(\theta_1-\theta_2+2\pi)}{G^{(1)}(\theta_1-\theta_2)} \equiv f_{\mathrm{R}}(t),\end{aligned} \tag{4.16}$$

where, the function $G^{(n)}(\theta)$ is the Green's function we obtain in the calculation of the corresponding scalar QFT. The angles θ_1 and θ_2 are the same quantities as described in figure 3.5. $G^{(n)}(\theta_1-\theta_2)$ is the Green's function of the neighbouring scalar operator on the same sheet, and $G^{(n)}(\theta_1-\theta_2+2\pi)$ is the Green's function of the neighbouring scalar operators on different sheets.

We call this algebra here, the *Finite Time Algebra* (FTA). We can show that in the late time limit $t \to \infty$, FTA is identical with the commutation relation of LTA given previously (4.6) for $C = 1$ case. Thus, FTA is an extension of LTA to finite time.

Correspondingly in the FTA the normalization for n-particle states must be changed as [1]

$$\begin{aligned}|n\rangle_{\mathrm{L}} &= (n! f_{\mathrm{L}}(t)^n)^{-\frac{1}{2}} \left(\hat{\phi}^{\mathrm{L}\dagger}\right)^n |0\rangle_{\mathrm{L}}, \\ |n\rangle_{\mathrm{R}} &= (n! f_{\mathrm{R}}(t)^n)^{-\frac{1}{2}} \left(\hat{\phi}^{\mathrm{R}\dagger}\right)^n |0\rangle_{\mathrm{R}}.\end{aligned} \tag{4.18}$$

[1] The normalization for $|1\rangle_{\mathrm{L}}$ and $|2\rangle_{\mathrm{L}}$ for example is:

$$\begin{aligned}{}_{\mathrm{L}}\langle 0|\hat{\phi}^{\mathrm{L}}\hat{\phi}^{\mathrm{L}\dagger}|0\rangle_{\mathrm{L}} &= f_{\mathrm{L}}(t), \\ {}_{\mathrm{L}}\langle 0|\hat{\phi}^{\mathrm{L}}\hat{\phi}^{\mathrm{L}}\hat{\phi}^{\mathrm{L}\dagger}\hat{\phi}^{\mathrm{L}\dagger}|0\rangle_{\mathrm{L}} &= 2! f_{\mathrm{L}}(t)^2.\end{aligned} \tag{4.17}$$

The Rényi EE of the effective density matrix with this commutation relation for each time slice is equivalent to the calculation performed by using the replica method in QFT at the same time slice.

Let us consider an effective state in FTA with one scalar operator, which corresponds to (4.11) in LTA,

$$\begin{aligned}|\psi^{\text{eff}}\rangle &= \mathcal{N} : \hat{\phi} : |0\rangle_{\text{L}} \otimes |0\rangle_{\text{R}} \\ &= \left(\left(\frac{f_{\text{L}}(t)}{f_{\text{L}}(t) + f_{\text{R}}(t)} \right)^{\frac{1}{2}} |1\rangle_{\text{L}} \otimes |0\rangle_{\text{R}} + \left(\frac{f_{\text{R}}(t)}{f_{\text{L}}(t) + f_{\text{R}}(t)} \right)^{\frac{1}{2}} |0\rangle_{\text{L}} \otimes |1\rangle_{\text{R}} \right).\end{aligned} \tag{4.19}$$

The effective reduced density matrix becomes

$$\begin{aligned}\rho_{\text{R}}^{\text{eff}} &= \text{tr}_{\text{L}} \left(|\psi^{\text{eff}}\rangle\langle\psi^{\text{eff}}| \right) \\ &= \frac{1}{f_{\text{L}}(t) + f_{\text{R}}(t)} \left(f_{\text{L}}(t) |0\rangle_{\text{RR}}\langle 0| + f_{\text{R}}(t) |1\rangle_{\text{RR}}\langle 1| \right),\end{aligned} \tag{4.20}$$

and thus the Rényi EE is

$$\begin{aligned}S_{\text{R}}^{(n),\text{LTA}} &= \frac{1}{1-n} \log \text{tr}_{\text{R}} \left[(\rho_{\text{R}}^{\text{eff}})^n \right] \\ &= \frac{1}{1-n} \log \left[\left(f_{\text{L}}(t) + f_{\text{R}}(t) \right)^{-n} \left(f_{\text{L}}(t)^n + f_{\text{R}}(t)^n \right) \right].\end{aligned} \tag{4.21}$$

which is exactly the same as we obtained from the QFT calculation for the excited state

$$|\psi^{\text{ex}}\rangle = \phi\left(-t, -\ell\right) |0\rangle. \tag{4.22}$$

Moreover, if we have a density matrix ρ in the form

$$\rho = P_1 |1\rangle\langle 1| + P_0 |0\rangle\langle 0| \tag{4.23}$$

where $|n\rangle$ is an n-particle state, P_1 and P_2 is the probability for the 1-particle state and 0-particle state, respectively.

Thus, the effective reduced density matrix in (4.20) suggests that we can describe this as a density matrix of a one-quasi-particle system. If we define P_{L} and P_{R} as

$$\begin{aligned} P_{\mathrm{L}} &= \left(\frac{f_{\mathrm{L}}(t)}{f_{\mathrm{L}}(t) + f_{\mathrm{R}}(t)} \right), \\ P_{\mathrm{R}} &= \left(\frac{f_{\mathrm{R}}(t)}{f_{\mathrm{L}}(t) + f_{\mathrm{R}}(t)} \right), \end{aligned} \tag{4.24}$$

then the effective reduced density matrix is expressed as

$$\rho_{\mathrm{R}}^{\mathrm{eff}} = P_{\mathrm{L}} |0\rangle_{\mathrm{RR}} \langle 0| + P_{\mathrm{R}} |1\rangle_{\mathrm{RR}} \langle 1|. \tag{4.25}$$

Therefore, we can understand P_{L} and P_{R} as the probability that we observe the quasi-particle on the left or right half of the system, respectively.

These functions $P_{\mathrm{L}}, P_{\mathrm{R}}$ have an interesting geometrical understanding in 4 dimensional spacetime, and that will be explained in the following section as the *particle propagating model* .

Another example using FTA for the operator insertion $: \hat{\phi}^k :$ is presented in the Appendix A.1.

4.4 Particle Propagating Model

In this section, we restrict the spacetime to 4 dimension and introduce the *Particle Propagating Model* (PPM).

Let us recall here the space decomposition that we defined for the QFT discussion in section 3.1. We have 4 dimensional spacetime $\mathbb{R}^4$, and the subspaces $\mathcal{A}$ and $\mathcal{B}$ are defined on the time slice $\mathcal{M}_0 = \{p \in \mathcal{M} | x^0(p) = 0\}$ as

$$\begin{aligned} \mathcal{A} &:= \{p \in \mathbb{R}^4 \mid x^1(p) \geqq 0, x^0(p) = 0\} \\ \mathcal{B} &:= \mathcal{A}^c = \{p \in \mathbb{R}^4 \mid x^1(p) < 0, x^0(p) = 0\} \end{aligned} \tag{4.26}$$

where $\mathcal{B}$ is the complement of the subspace $\mathcal{A}$ on the time slice $\mathcal{M}_0$. The entangling surface Σ is the boundary of the subspaces $\mathcal{A}$ and $\mathcal{B}$,

$$\Sigma := \{p \in \mathbb{R}^4 | x^0(p) = 0, x^1(p) = 0\}. \tag{4.27}$$

In the QFT calculation, we have inserted a spacetime local field operator ϕ at the point $(-t, -\ell)$. On the other hand in the PPM, we assume that a free massless quasi-particle is created at the point $(-t, -\ell)$ with the operator insertion. Since the quasi-particle is massless, it propagates at the speed of light. Thus, the propagation of the particle is on the sphere with radius t in $\mathcal{M}_0$. We define this sphere as $\mathcal{K}$,

$$\mathcal{K} := \{p \in \mathbb{R}^4 | \left(x^1(p) + \ell\right)^2 + \left(x^2(p)\right)^2 + \left(x^3(p)\right)^2 = t^2, x^0(p) = 0\}. \tag{4.28}$$

As in the case for QFT, according to the insertion time t there are 4-cases as follows,

(i) At the time $t < \ell$, where $\mathcal{K} \subset \mathcal{B}$.

(ii) At the time $t = \ell$, where the sphere $\mathcal{K}$ touches the entangling surface Σ.

(iii) At the time $t > \ell$, where $\mathcal{K}$ is shared with $\mathcal{A}$ and $\mathcal{B}$.

(iv) At the time $t = \infty$, where the two subspaces $\mathcal{A}$ and $\mathcal{B}$ divide the sphere $\mathcal{K}$ into half.

The labels (i) and (iii) corresponds to the labels in figure 4.2 (a) and (b), respectively.

We assume here that the probability to find the particle at some point on the sphere $\mathcal{K}$ is equal everywhere on it. Then, the probability $P_{\mathcal{A}}$, $P_{\mathcal{B}}$ to detect the particle in the subregion $\mathcal{A}$, $\mathcal{B}$, respectively, can be evaluated from the surface area of the sphere $\mathcal{K}$: The total surface area of the sphere is $4\pi t^2$. The area of the sphere

$\mathcal{K}$ included in $\mathcal{B}$ at $t \geqq \ell$ is $2\pi t(t-\ell)$. Thus the probability of $P_{\mathcal{A}}$ and $P_{\mathcal{B}}$ to detect the particle becomes,

$$(P_{\mathcal{A}}(t,\ell), P_{\mathcal{B}}(t,\ell)) = \begin{cases} (0,1) & t < \ell \\ (\frac{t+\ell}{2t}, \frac{t-\ell}{2t}) & t \geqq \ell \end{cases}. \tag{4.29}$$

We found that these probabilities $P_{\mathcal{A}}$ and $P_{\mathcal{B}}$ are equivalent with P_{L} and P_{R} in equation (4.25) of 4 dimensional free scalar QFT.

To generalize this PPM for multi-particle case, we assume that:

- *One* local operator creates *one* quasi-particle.
- Quasi-particles created at the *same* point of spacetime *cannot be distinguished*.

Note that the second assumption also means that we *distinguish* quasi-particles created at different points in spacetime. The basis of the Hilbert space is labeled by the number of particles found in subregions $\mathcal{A}$ and $\mathcal{B}$. For example, if we have n different insertion points, that means we have n kinds of particle to distinguish. Then we write the number of these particles located in subregion $\mathcal{A}$ as $(a_1, a_2, \cdots, a_n)$ and subregion $\mathcal{B}$ as $(b_1, b_2, \cdots, b_n)$, where the lower indices are the label for the kind of quasi particle. Then, we write such a state as $|a_1, a_2, \cdots, a_n; b_1, b_2, \cdots, b_n\rangle$, with an appropriate normalization. The Hilbert space is spanned by these states:

$$\mathscr{H}_{\mathrm{PPM}} = \mathrm{Span}\{|a_1, a_2, \cdots, a_n; b_1, b_2, \cdots, b_n\rangle\}. \tag{4.30}$$

Under these assumptions, we define the density matrix ρ^{PPM} and the Rényi Entropy $S^{(n),\mathrm{PPM}}$ as follows. The Rényi Entropy $S^{(n),\mathrm{PPM}}$ is defined by

$$S^{(n),\mathrm{PPM}} = \begin{cases} \frac{1}{1-n} \log \mathrm{tr}\left((\rho^{\mathrm{PPM}})^n\right) & n \geqq 2 \\ -\mathrm{tr}\left(\rho^{\mathrm{PPM}} \log \rho^{\mathrm{PPM}}\right) & n = 1 \end{cases}. \tag{4.31}$$

as usual, where ρ^{PPM} is constructed depending on the number and location of the particles (see examples below and in the appendix A.2).

As a result, the obtained Rényi Entropy $S^{(n),\text{PPM}}$ is equivalent to the Rényi EE growth $\Delta S_{\mathcal{A}}^{(n)}$ in 4 dimensional spacetime free scalar QFT:

$$S^{(n),\text{PPM}} = \Delta S_{\mathcal{A}}^{(n)}. \tag{4.32}$$

Let us give the example with one scalar operator insertion at $(-t, -l)$. In this case, the density matrix ρ^{PPM} is

$$\rho^{\text{PPM}} = P_{\mathcal{A}}(t,\ell)|1;0\rangle\langle 1;0| + P_{\mathcal{B}}(t,\ell)|0;1\rangle\langle 0;1|, \tag{4.33}$$

since the probability to find the quasi-particle in subregion $\mathcal{A}$ or $\mathcal{B}$ is $P_{\mathcal{A}}(t,\ell)$ or $P_{\mathcal{B}}(t,\ell)$, respectively. The Rényi Enropy of this density matrix for $n \geqq 2$ is then

$$S^{(n),\text{PPM}} = \frac{1}{1-n}\log\left(P_{\mathcal{A}}(t,\ell)^n + P_{\mathcal{B}}(t,\ell)^n\right) \tag{4.34}$$

$$= \begin{cases} 0 & t < \ell \\ \frac{1}{1-n}\log\left(\left(\frac{t-\ell}{2t}\right)^n + \left(\frac{t-\ell}{2t}\right)^n\right) & t \geqq \ell \end{cases}, \tag{4.35}$$

which agrees with the QFT result perfectly.

By using this model, we can evaluate the Rényi EE growth $\Delta S_{\mathcal{A}}^{(n)}$ or other quantities such as the growth of mutual information in more complicated space decompositions that are difficult to handle in QFT. More examples can be found in Appendix A.2.

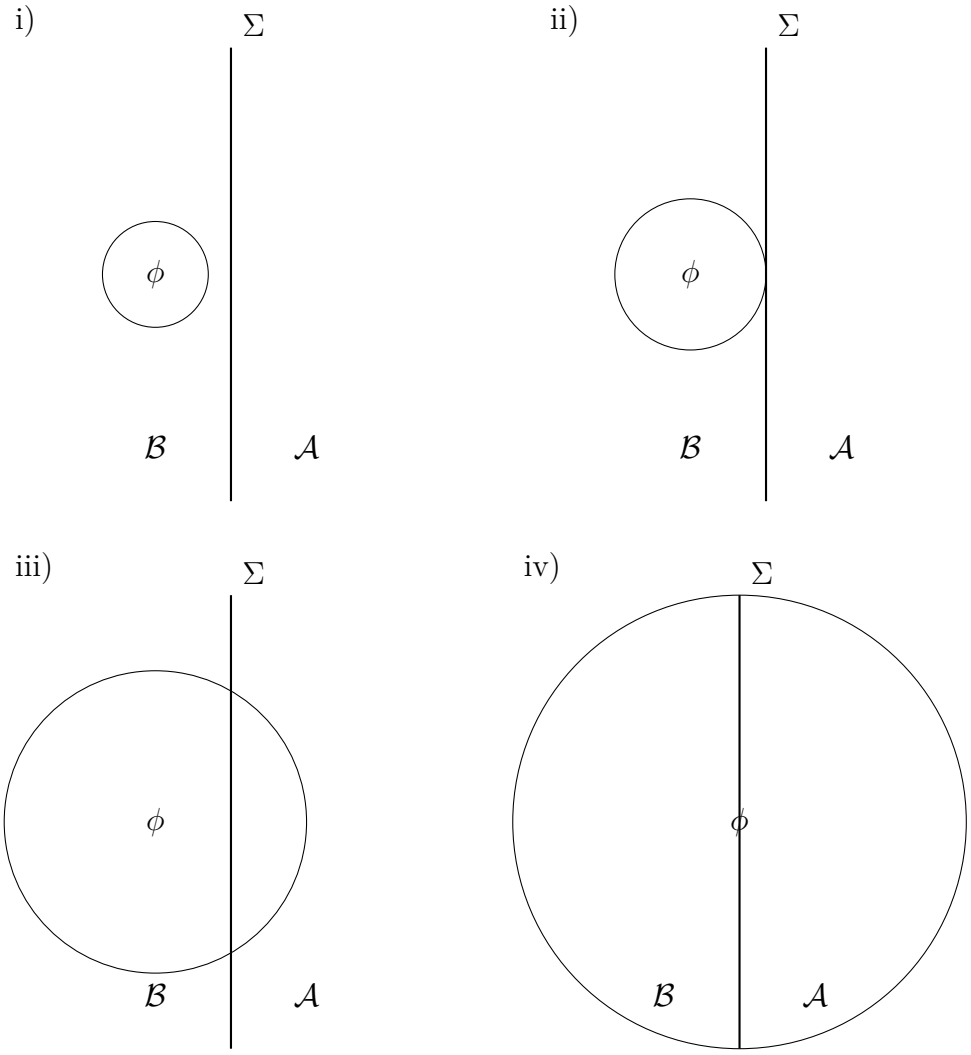

Figure 4.1: Schematic picture of the propagation of the effect by an inserted operator. The line in the middle is the entangling surface Σ that divides the space into subregions $\mathcal{A}$ and $\mathcal{B}$, the circle is the front of the propagating effect by the inserted operator, and the position of the inserted operator is shown as ϕ. The 4 figures decribes the picture at the following time: i) $0 \leqq t < \ell$, ii) $t = \ell$, iii) $t > \ell$, iv) $t = \infty$.

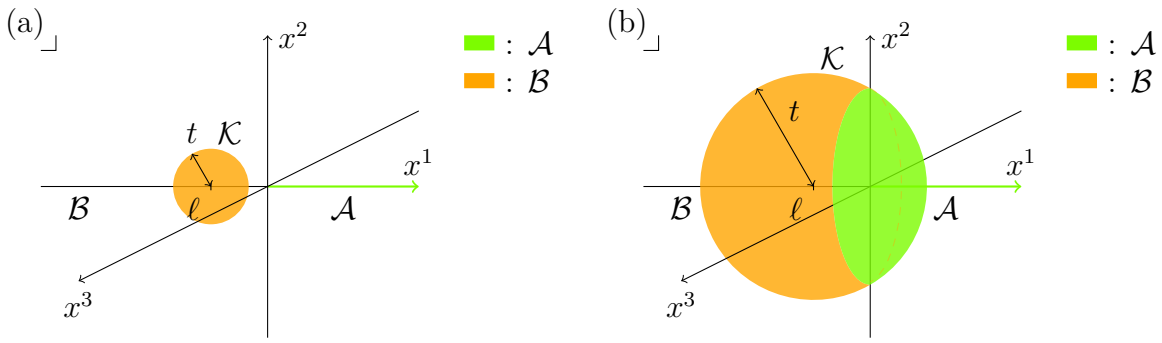

Figure 4.2: Picture of the sphere $\mathcal{K}$ at two parameter regions. Figure (a) shows the sphere $\mathcal{K}$ at $t < \ell$, figure (b) shows the sphere $\mathcal{K}$ at $t \geqq \ell$. The orange and green part of sphere $\mathcal{K}$ belongs to subregion $\mathcal{A}$ and $\mathcal{B}$, respectively.

Chapter 5

Growth of Rényi EE for Maxwell Theory

In this chapter, we study the Rényi EE growth $\Delta S_{\mathcal{A}}^{(n)}$ for Maxwell theory in 4 and higher even dimensional spacetime. The EE of gauge theory is not well defined since it is not gauge invariant. However, as we discuss in this section, the Rényi EE growth $\Delta S_{\mathcal{A}}^{(n)}$ for locally excited states can be defined in a gauge invariant manner. Thus, in spite of the problem of defining the Rényi EE for gauge fields, we are able to discuss the entanglement of gauge fields in terms of its growth.

We will first formally derive the Rényi EE growth $\Delta S_{\mathcal{A}}^{(n)}$ for Maxwell fields, and then discuss the gauge independence.

5.1 Space Decomposition and Lagrangian

The spacetime and its decomposition are the same as we have performed for scalar fields. We consider a $d+1$-dimensional flat spacetime $\mathcal{M} = \mathbb{R}^{d+1}$, where d is an odd number that is 3 or larger. The subregions $\mathcal{A}, \mathcal{B}$ are taken in the same way as

previously:

$$\mathcal{A} = \{p \in \mathcal{M}_0 | x^1(p) \geqq 0\}, \tag{5.1}$$

$$\mathcal{B} = \mathcal{A}^c. \tag{5.2}$$

The Lagrangian we consider here is the free Maxwell theory with Faddeev-Popov ghosts b, c,

$$\mathscr{L} = -\frac{1}{4}F^{\mu\nu}F_{\mu\nu} - \partial^\mu b A_\mu + \frac{\alpha}{2}b^2 - i\partial^\mu \bar{c}\partial_\mu c, \tag{5.3}$$

where $F_{\mu\nu} = \partial_\mu A_\nu - \partial_\nu A_\mu$, and A_μ is real valued (i.e. $A_\mu \in \mathbb{R}$). This is the Lagrangian for a free Maxwell field with gauge fixing parameter α. The equations of motion for the fields are

$$\partial^\nu \partial_\nu A_\mu = (1-\alpha)\partial_\mu b, \tag{5.4}$$

$$\partial^\mu \partial_\mu b = 0. \tag{5.5}$$

We choose the gauge fixing parameter $\alpha = 1$, which means that we take the Feynman gauge. Then, A_μ obeys the Klein-Gordon equation of motion, and the Green's function of A_μ is proportional to that of scalar field.

5.2 The Green's Function

The locally excited state we want to discuss, should be gauge invariant. Thus the operator we want to insert is $F_{\mu\nu}$. In 4 dimensional Euclidean spacetime, they are combinations of the electric field $\mathbf{E}_i$ and magnetic field $\mathbf{B}_i$,

$$\mathbf{E}_i = -iF_{0i} \tag{5.6}$$

$$\mathbf{B}_i = -\frac{1}{2}\varepsilon_{ijk}F^{jk}, \tag{5.7}$$

where $i, j, k \in \{1, 2, 3\}$, and ε_{ijk} is the completely antisymmetric tensor with $\varepsilon_{123} = 1$. The operator are inserted at the same point like in the scalar field case, as described in figure 3.5.

The Green's function for the gauge invariant operators are derived as the derivatives of Green's functions of A_μ. For example in 4-dimensional spacetime, $\mathbf{E}_i$ is derived from the propagator $\langle A_\mu A_\nu \rangle$ as

$$\begin{aligned}
\langle \mathbf{E}_i^\dagger \mathbf{E}_j \rangle &= -\langle F_{0i} F_{0j} \rangle \\
&= -\langle (\partial_0 A_i - \partial_i A_0)(\partial_0 A_j - \partial_j A_0) \rangle \\
&= -\langle \partial_0 A_i \partial_0 A_j \rangle - \langle \partial_i A_0 \partial_j A_0 \rangle + \langle \partial_i A_0 \partial_0 A_j \rangle + \langle \partial_0 A_i \partial_j A_0 \rangle \\
&= -\partial_0 \partial_0 \langle A_i A_j \rangle - \partial_i \partial_j \langle A_0 A_0 \rangle + \partial_i \partial_0 \langle A_0 A_j \rangle + \partial_0 \partial_j \langle A_i A_0 \rangle
\end{aligned} \tag{5.8}$$

where in the last line, the order of differential operator acts on each vector field A_μ, as $\partial_\mu \partial_\nu \langle A_\rho A_\sigma \rangle = \frac{\partial}{\partial x^\mu} \frac{\partial}{\partial y^\nu} \langle A_\rho(x) A_\sigma(y) \rangle$. The Green's function for the magnetic field $\mathbf{B}_i$ is obtained by,

$$\begin{aligned}
\langle \mathbf{B}_i^\dagger \mathbf{B}_l \rangle &= \frac{1}{4} \varepsilon_{ijk} \varepsilon_{lmn} \langle \left(\partial^j A^k - \partial^k A^j \right) (\partial^m A^n - \partial^n A^m) \rangle \\
&= \frac{1}{4} \varepsilon_{ijk} \varepsilon_{lmn} \left(\partial^j \partial^m \langle A^k A^n \rangle + \partial^k \partial^n \langle A^j A^m \rangle - \left(\partial^j \partial^n \langle A^k A^m \rangle + \partial^k \partial^m \langle A^j A^n \rangle \right) \right)
\end{aligned} \tag{5.9}$$

where in the last line we use again the notation $\partial_\mu \partial_\nu \langle A_\rho A_\sigma \rangle = \frac{\partial}{\partial x^\mu} \frac{\partial}{\partial y^\nu} \langle A_\rho(x) A_\sigma(y) \rangle$.

The leading term in the ϵ dependence of the Green's functions for $d = 3, 5$ are summarized in the Appendix B.1.

5.3 Gauge Fixing and Gauge Invariance

The EE of gauge theory depends on the regularization scheme [8, 29, 30, 31]. It was pointed out that in lattice gauge theory [17] this is due to the assumption that we can decompose the Hilbert space. The gauge invariant Hilbert space does not admit the decomposition into a tensor product of two gauge invariant subspaces associated with subregions $\mathcal{A}$ and $\mathcal{B}$:

$$\mathscr{H}^{\text{inv}} \neq \mathscr{H}_{\mathcal{A}}^{\text{inv}} \otimes \mathscr{H}_{\mathcal{B}}^{\text{inv}}, \tag{5.10}$$

due to the Gauss law constraint. This makes it impossible to define the reduced density matrix in a gauge invariant way. The so-called extended Hilbert space was introduced, that is an extension of the Hilbert space $\mathscr{H}^{\rm inv}$ that also includes non gauge invariant states, and admits the tensor product decomposition. In [17], it was also mentioned that in 1 dimensional lattice, if we fix the gauge on the entangling surface Σ, the result depends on gauge choice.

In continuum theory, it was shown that the difference in the results can be understood as the EE of edge modes that are living on the entangling surface Σ [16].

Here, we discuss the gauge dependence of the Rényi EE growth $\Delta S_{\mathcal{A}}^{(n)}$. We assume, that the subtlety in gauge theory is due to the decomposition of Hilbert space, and the effect of gauge choice appears on the boundary as the boundary condition. Under this assumption, we show that the Rényi EE growth $\Delta S_{\mathcal{A}}^{(n)}$ does not depend on the boundary condition and thus we have not to worry about this subtlety.

We start by considering the following path integral,

$$Z_1^{BC} = \int \mathcal{D}\phi \; e^{-\int d^4x (\partial_\mu \phi \partial^\mu \phi)} \delta(\phi - \phi_0), \tag{5.11}$$

where Z_n^{BC} is the partition function on $\mathcal{M}^{(n)}$ with boundary condition, ϕ_0 is the boundary condition at the entangling surface Σ. We can exponentiate the delta function and include it in the path integral as

$$Z_1^{BC} = \int \mathcal{D}\phi \mathcal{D}c \mathcal{D}\bar{c} \; e^{-\int d^4x \left(\partial_\mu \phi^\dagger(x) \partial^\mu \phi(x)\right) + i \int d^3\tilde{x} \left[c(\tilde{x})(\phi(\tilde{x}) - \phi_0(\tilde{x})) + \bar{c}(\tilde{x}) \left(\phi^\dagger(\tilde{x}) - \phi_0^\dagger(\tilde{x})\right)\right]}, \tag{5.12}$$

where $\tilde{x}^{(k)}$ is the coordinate on Σ on the k-th sheet.

We are interested in the $2n$-point functions on the n-sheeted manifold $\mathcal{M}^{(n)}$. With this new action, the $2n$-point function in the case with boundary condition

$\langle\left(\phi^\dagger\left(-t,-\ell\right)\phi\left(-t,-\ell\right)\right)^n\rangle_{BC}$ becomes

$$
\begin{aligned}
&\langle\left(\phi^\dagger\left(-t,-\ell\right)\phi\left(-t,-\ell\right)\right)^n\rangle_{BC}\\
&=\int\mathcal{D}\phi\int\mathcal{D}^n c\mathcal{D}^n\bar{c}\left(\phi^\dagger\left(-t,-\ell\right)\phi\left(-t,-\ell\right)\right)^n e^{-\int d^4x\partial_\mu\phi^\dagger\partial^\mu\phi+\sum_{k=1}^n c_k(x)(\phi(x)-\phi_0(x))+\bar{c}_k(x)\left(\phi^\dagger(x)-\phi_0^\dagger(x)\right)}\\
&=\int\mathcal{D}\phi\mathcal{D}^n c\mathcal{D}^n\bar{c}\left(\phi^\dagger\left(-t,-\ell\right)\phi\left(-t,-\ell\right)\right)^n e^{-\int d^4x\partial_\mu\phi^\dagger\partial^\mu\phi+\int d^3\tilde{x}\ \sum_{k=1}^n c_k(\tilde{x})(\phi(\tilde{x})-\phi_0(\tilde{x}))+\bar{c}_k(\tilde{x})\left(\phi^\dagger(\tilde{x})-\phi_0^\dagger(\tilde{x})\right)}\\
&=\int\mathcal{D}\phi\left(\phi^\dagger\left(-t,-\ell\right)\phi\left(-t,-\ell\right)\right)^n e^{-\int d^4x\partial_\mu\phi^\dagger\partial^\mu\phi-\int d^3(\tilde{x}^{(k)}c_k(\tilde{x})\phi_0+\bar{c}_k(\tilde{x})\phi_0^\dagger)}\\
&\qquad\left(1+\sum_{s=1}^\infty\frac{1}{s!}:\left(\int d^3\tilde{x}^{(k)}\ \sum_{k=1}^n c_k(\tilde{x}^{(k)})\phi(\tilde{x}^{(k)})+\bar{c}_k(\tilde{x}^{(k)})\phi^\dagger(\tilde{x}^{(k)})\right)^s:\right)\\
&=\mathcal{C}^n\langle\left(\phi^\dagger\left(-t,-\ell\right)\phi\left(-t,-\ell\right)\right)^n\rangle+\sum_{s=1}^\infty\frac{1}{s!}\left\langle\mathcal{C}^n\left(\phi^\dagger\phi\right)^n:\int d^{3s}\tilde{x}\mathcal{F}^{(s)}\left(\phi(\tilde{x}),\phi^\dagger(\tilde{x})\right):\right\rangle,
\end{aligned}
\tag{5.13}
$$

where $\mathcal{C}=\int\mathcal{D}c\mathcal{D}\bar{c}e^{\int d^3\tilde{x}c(\tilde{x})\phi_0(\tilde{x})+\bar{c}(\tilde{x})\phi_0(\tilde{x})}$ on each sheet, and $\mathcal{F}^{(s)}$ is a homogeneous polynomial function of order s in $c(\tilde{x}^{(k)})\phi(\tilde{x}^{(k)})$ and $\bar{c}(\tilde{x}^{(k)})\phi^\dagger(\tilde{x}^{(k)})$ with combinatorial factors. In the last line of equation (5.13), the second term on the right hand side can be understood as the correction to the result without boundary condition. The first term is identical with the result without boundary condition, and the second term works as the correction to it.

By an explicit calculation, this correlation function of the operator on the boundary $\phi(\tilde{x})$ with the inserted operator $\phi\left(-t,-\ell\right)$ is not divergent in the limit $\epsilon\to 0$. Thus, for example in $d=3$ case, where we have 4 spacetime dimensions, we get

$$
\langle\left(\mathcal{O}^\dagger\mathcal{O}\right)^n\rangle_{\mathrm{BC}}=\mathcal{C}^n\langle\left(\mathcal{O}^\dagger\mathcal{O}\right)^n\rangle+O(\epsilon^{-3n}),
\tag{5.14}
$$

where the leading term's divergence is $O(\epsilon^{-4n})$, and all the corrections are included in $O(\epsilon^{-3n})$.

This means that the effect of boundary does not affect the result. As we have

seen in (2.50), the final result is

$$\begin{aligned}\Delta S_{\mathcal{A}}^{(n)} &= -\frac{1}{1-n}\log\frac{\langle(\mathcal{O}^\dagger\mathcal{O})^n\rangle_{\Sigma_n,\,\mathrm{BC}}}{\left(\langle\mathcal{O}^\dagger\mathcal{O}\rangle_{\Sigma_1,\,\mathrm{BC}}\right)^n} \\ &= -\frac{1}{1-n}\log\frac{\mathcal{C}^n\epsilon^{4n}\langle\left(\mathcal{O}^\dagger\mathcal{O}\right)^n\rangle_{\Sigma_n}+\epsilon^{4n}O(\epsilon^{-3n})}{\epsilon^{4n}\left(\mathcal{C}\langle\mathcal{O}^\dagger\mathcal{O}\rangle_{\Sigma_1}+O(\epsilon^{-3})\right)^n}\end{aligned} \tag{5.15}$$

and since the corrections from the boundary are all depending weaker on ϵ than $-4n$, in the limit $\epsilon \to 0$ all the correction terms vanish and $\mathcal{C}$ cancels. Thus these corrections do not appear in the final result.

5.4 Time Evolution of the Rényi EE Growth $\Delta S_{\mathcal{A}}^{(n)}$

We have analyzed the time evolution of $\Delta S_{\mathcal{A}}^{(n)}$ in several cases. We will summarize the results here. In this section, we denote the Rényi EE growth for the inserted operator $\mathcal{O}$ as $\Delta S_{\mathcal{A}}^{(n)}[\mathcal{O}]$,

We start with the most simple case, when only one operator $\mathbf{E}_i$ or $\mathbf{B}_i$ is inserted. The resulting Rényi EE growth $\Delta S_{\mathcal{A}}^{(n)}$ for $\mathbf{E}_1$ and $\mathbf{E}_2$ are,

$$\Delta S_{\mathcal{A}}^{(n)}[\mathbf{E}_1] = \frac{1}{1-n}\log\left(\left(-\frac{(t+\ell)^2(2t-\ell)}{4t^3}\right)^n+\left(\frac{(t-\ell)^2(2t+\ell)}{4t^3}\right)^n\right), \tag{5.16}$$

$$\Delta S_{\mathcal{A}}^{(n)}[\mathbf{E}_2] = \frac{1}{1-n}\log\left(\left(\frac{4t^3-3\ell t^2-\ell^3}{8t^3}\right)^n+\left(\frac{4t^3+3\ell t^2+\ell^3}{8t^3}\right)^n\right), \tag{5.17}$$

respectively. For the other operators we find the following relations,

$$\Delta S_{\mathcal{A}}^{(n)}[\mathbf{E}_1] = \Delta S_{\mathcal{A}}^{(n)}[\mathbf{B}_1], \tag{5.18}$$

$$\Delta S_{\mathcal{A}}^{(n)}[\mathbf{E}_2] = \Delta S_{\mathcal{A}}^{(n)}[\mathbf{E}_3] = \Delta S_{\mathcal{A}}^{(n)}[\mathbf{B}_2] = \Delta S_{\mathcal{A}}^{(n)}[\mathbf{B}_3]. \tag{5.19}$$

We plotted their 2nd Rényi EE growth in figure 5.1, where the horizontal axis is $\frac{t}{\ell}$, and the vertical axis is $\Delta S_{\mathcal{A}}^{(2)}$. We can see that for both functions the growth is zero until $t=\ell$, but differs after $t=\ell$. Just after $t=\ell$, the Rényi EE for $\mathbf{E}_2$ or $\mathbf{E}_3$ grows faster than the one for $\mathbf{E}_1$.

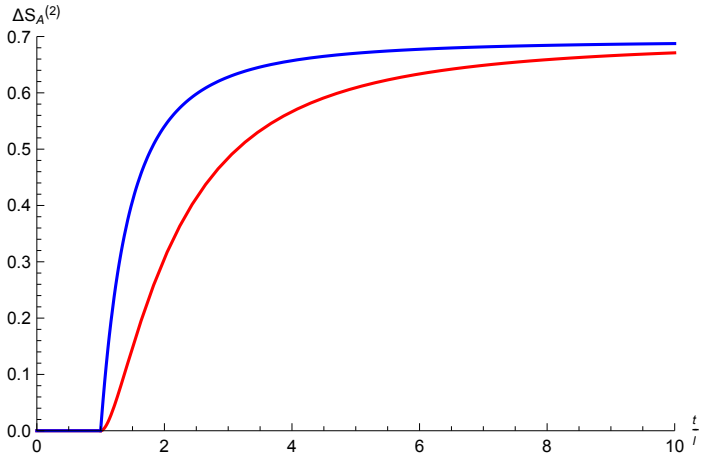

Figure 5.1: Plot of $\Delta S_{\mathcal{A}}^{(2)}\,[\mathbf{E}_1]$ and $\Delta S_{\mathcal{A}}^{(2)}\,[\mathbf{E}_2]$ which correspond to red and blue lines, respectively.

This behaviour can be understood from classical electromagnetism. Classically, electromagnetic waves are transverse waves and thus have no component in the direction they travel. In the present case, an electromagnetic wave that is traveling towards the entangling surface Σ has no component in $\mathbf{E}_1$. It can only have non-zero components in $\mathbf{E}_2$ or $\mathbf{E}_3$.

In QFT on the other hand, by acting with an operator such as $\mathbf{E}_1$ or $\mathbf{E}_2$ on the vacuum, we are exciting the field in a specific direction. Thus the change of Rényi EE by inserting $\mathbf{E}_1$ is growing slower than the one by inserting $\mathbf{E}_2$ or $\mathbf{E}_3$. See figure 5.1, where the blue line is the $\mathbf{E}_2$ insertion and red line is the $\mathbf{E}_1$ insertion. The time evolution for $\mathbf{E}_1$ and $\mathbf{B}_1$ are the same, and the time evolution for $\mathbf{E}_2$, $\mathbf{E}_3$, $\mathbf{B}_2$, $\mathbf{B}_3$ are the same. This shows that the result has the rotation symmetry as expected, and also the electromagnetic duality is preserved.

In the late time limit $t \to \infty$, all the cases of single operator insertion considered above converge to the same value $\log 2$. In fact, this is true for all integers n in this case, even for the limit $n \to 1$, where we obtain the EE growth:

$$\lim_{t\to\infty} \Delta S_{\mathcal{A}}^{(n)}\,[\mathbf{E}_i] = \log 2\ , \tag{5.20}$$

$$\lim_{t\to\infty} \Delta S_{\mathcal{A}}^{(n)}\,[\mathbf{B}_i] = \log 2\ , \tag{5.21}$$

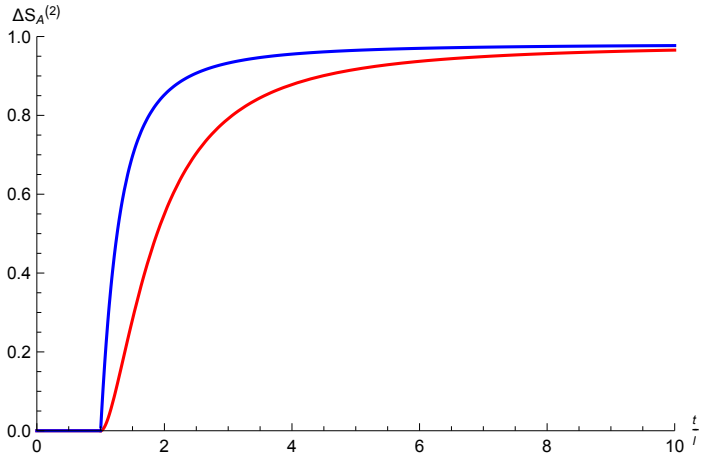

Figure 5.2: Rényi EE growth for $\mathbf{E}_1^2$ and $\mathbf{E}_2^2$ insertion. The red and blue lines are $\Delta S_{\mathcal{A}}^{(2)}\left[{\mathbf{E}_1}^2\right]$ and $\Delta S_{\mathcal{A}}^{(2)}\left[{\mathbf{E}_2}^2\right]$, respectively.

where $i = 1, 2, 3$.

Figure 5.2 shows the 2nd Réyni EE growth for the insertion of $\mathbf{E}_1^2$ and $\mathbf{E}_2^2$. Their explicit functions look as follows;

$$\Delta S_{\mathcal{A}}^{(n)}\left[\mathbf{E}_1^2\right] = \frac{1}{1-n}\log\left[\left(\frac{(2t-\ell)\,(t+l)^2}{4t^3}\right)^{2n} + \left(\frac{(2t+\ell)(t-l)^2}{4t^3}\right)^{2n} + 2^n\left(\frac{(2t-\ell)\,(t+\ell)^2}{4t^3}\right)^{n}\left(\frac{(2t+\ell)(t-l)^2}{4t^3}\right)^{n}\right], \tag{5.22}$$

$$\Delta S_{\mathcal{A}}^{(n)}\left[\mathbf{E}_2^2\right] = \frac{1}{1-n}\log\left[\left(\frac{4t^3+3\ell t^2+\ell^3}{8t^3}\right)^{2n} + \left(\frac{4t^3-3\ell t^2-\ell^3}{8t^3}\right)^{2n} + 2^n\left(\frac{4t^3+3\ell t^2+\ell^3}{8t^3}\right)^{n}\left(\frac{4t^3-3\ell t^2-\ell^3}{8t^3}\right)^{n}\right], \tag{5.23}$$

where the Rényi EE growth for $\mathbf{B}_i^2$ insertion is the same as the growth for $\mathbf{E}_i^2$ insertion. Here, we can see again that the behaviour is similar to an insertion of a single operator like $\mathbf{E}_1$ or $\mathbf{E}_2$. However, their late time limit is more complicated,

and depends on n:

$$\lim_{t\to\infty} \Delta S_{\mathcal{A}}^{(n)} \left[\mathbf{E}_i^2\right] = \frac{1}{1-n} \log\left(2^{1-2n} + 2^{-n}\right) \tag{5.24}$$

where $n \geqq 2$. In the limit $n \to 1$ this gives

$$\lim_{t\to\infty} \Delta S_{\mathcal{A}}^{(1)} \left[\mathbf{E}_i^2\right] = \frac{3}{2} \log 2. \tag{5.25}$$

They agree with the result of free scalar field ϕ^2 insertion.

5.5 Late Time Algebra and Finite Time Algebra

In this section, we introduce the Late Time Algebra (LTA) for the Maxwell theory.

The construction of LTA for Maxwell theory works in the same way as for scalar field theory. First, we introduce the following LTA operators

$$\hat{\mathbf{E}}_i^{\mathrm{L}}, \hat{\mathbf{E}}_i^{\mathrm{L}\dagger}, \hat{\mathbf{E}}_i^{\mathrm{R}}, \hat{\mathbf{E}}_i^{\mathrm{R}\dagger}, \hat{\mathbf{B}}_i^{\mathrm{L}}, \hat{\mathbf{B}}_i^{\mathrm{L}\dagger}, \hat{\mathbf{B}}_i^{\mathrm{R}}, \hat{\mathbf{B}}_i^{\mathrm{R}\dagger} \tag{5.26}$$

and their linear combinations

$$\hat{\mathbf{E}}_i = \hat{\mathbf{E}}_i^{\mathrm{L}} + \hat{\mathbf{E}}_i^{\mathrm{L}\dagger} + \hat{\mathbf{E}}_i^{\mathrm{R}} + \hat{\mathbf{E}}_i^{\mathrm{R}\dagger}, \tag{5.27}$$

$$\hat{\mathbf{B}}_i = \hat{\mathbf{B}}_i^{\mathrm{L}} + \hat{\mathbf{B}}_i^{\mathrm{L}\dagger} + \hat{\mathbf{B}}_i^{\mathrm{R}} + \hat{\mathbf{B}}_i^{\mathrm{R}\dagger}. \tag{5.28}$$

where L and R corresponds to the left and right moving mode. The commutation relations are defined from the Green's function of the corresponding fields. They are obtained as

$$\begin{aligned}
\left[\hat{\mathbf{E}}_i^{\mathrm{L}}, \hat{\mathbf{E}}_j^{\mathrm{L}\dagger}\right] &= \lim_{t\to\infty} 2\frac{\langle \mathbf{E}_i \mathbf{E}_j \rangle_{\mathcal{M}^{(n)}} (\theta_1 - \theta_2)}{\langle \mathbf{E}_1 \mathbf{E}_1 \rangle_{\mathcal{M}^{(1)}} (\theta_1 - \theta_2)}, \\
\left[\hat{\mathbf{E}}_i^{\mathrm{R}}, \hat{\mathbf{E}}_j^{\mathrm{R}\dagger}\right] &= \lim_{t\to\infty} 2\frac{\langle \mathbf{E}_i \mathbf{E}_j \rangle_{\mathcal{M}^{(n)}} (\theta_1 - \theta_2 + 2\pi)}{\langle \mathbf{E}_1 \mathbf{E}_1 \rangle_{\mathcal{M}^{(1)}} (\theta_1 - \theta_2)}, \\
\left[\hat{\mathbf{B}}_i^{\mathrm{L}}, \hat{\mathbf{B}}_j^{\mathrm{L}\dagger}\right] &= \lim_{t\to\infty} 2\frac{\langle \mathbf{B}_i \mathbf{B}_j \rangle_{\mathcal{M}^{(n)}} (\theta_1 - \theta_2)}{\langle \mathbf{E}_1 \mathbf{E}_1 \rangle_{\mathcal{M}^{(1)}} (\theta_1 - \theta_2)}, \\
\left[\hat{\mathbf{B}}_i^{\mathrm{L}}, \hat{\mathbf{B}}_j^{\mathrm{L}\dagger}\right] &= \lim_{t\to\infty} 2\frac{\langle \mathbf{B}_i \mathbf{B}_j \rangle_{\mathcal{M}^{(n)}} (\theta_1 - \theta_2 + 2\pi)}{\langle \mathbf{E}_1 \mathbf{E}_1 \rangle_{\mathcal{M}^{(1)}} (\theta_1 - \theta_2)},
\end{aligned} \tag{5.29}$$

where $\langle \mathbf{E}_i \mathbf{E}_j \rangle_{\mathcal{M}^{(n)}}(\theta_1 - \theta_2)$ is the propagator of neighboring operators on the same sheet, and $\langle \mathbf{E}_i \mathbf{E}_j \rangle_{\mathcal{M}^{(n)}}(\theta_1 - \theta_2 + 2\pi)$ is the propagator of neighboring operators on different sheets, similar to the schematic picture given in figure 3.7. A remarkable property in the LTA of Maxwell theory is the non-zero commutators of $\hat{\mathbf{E}}_2, \hat{\mathbf{B}}_3$ and $\hat{\mathbf{E}}_3 \hat{\mathbf{B}}_2$. This mixing in the commutator is the most significant difference from the LTA of scalar fields:

$$\left[\hat{\mathbf{E}}_2^{\mathrm{L}}, \hat{\mathbf{B}}_3^{\mathrm{L}\dagger}\right] = \lim_{t\to\infty} 2\frac{\langle \mathbf{E}_2 \mathbf{B}_3 \rangle_{\mathcal{M}^{(n)}}(\theta_1 - \theta_2)}{\langle \mathbf{E}_1 \mathbf{E}_1 \rangle_{\mathcal{M}^{(1)}}(\theta_1 - \theta_2)} \neq 0 \tag{5.30}$$

$$\left[\hat{\mathbf{E}}_2^{\mathrm{R}}, \hat{\mathbf{B}}_3^{\mathrm{R}\dagger}\right] = \lim_{t\to\infty} 2\frac{\langle \mathbf{E}_2 \mathbf{B}_3 \rangle_{\mathcal{M}^{(n)}}(\theta_1 - \theta_2 + 2\pi)}{\langle \mathbf{E}_1 \mathbf{E}_1 \rangle_{\mathcal{M}^{(1)}}(\theta_1 - \theta_2)} \neq 0 \tag{5.31}$$

$$\left[\hat{\mathbf{E}}_3^{\mathrm{L}}, \hat{\mathbf{B}}_2^{\mathrm{L}\dagger}\right] = \lim_{t\to\infty} 2\frac{\langle \mathbf{E}_3 \mathbf{B}_2 \rangle_{\mathcal{M}^{(n)}}(\theta_1 - \theta_2)}{\langle \mathbf{E}_1 \mathbf{E}_1 \rangle_{\mathcal{M}^{(1)}}(\theta_1 - \theta_2)} \neq 0 \tag{5.32}$$

$$\left[\hat{\mathbf{E}}_3^{\mathrm{R}}, \hat{\mathbf{B}}_2^{\mathrm{R}\dagger}\right] = \lim_{t\to\infty} 2\frac{\langle \mathbf{E}_3 \mathbf{B}_2 \rangle_{\mathcal{M}^{(n)}}(\theta_1 - \theta_2 + 2\pi)}{\langle \mathbf{E}_1 \mathbf{E}_1 \rangle_{\mathcal{M}^{(1)}}(\theta_1 - \theta_2)} \neq 0 \tag{5.33}$$

The Hilbert space is defined as the Fock space of these operators,

$$\mathscr{H}_{\mathrm{L}} = \mathrm{Span}\{|0\rangle_{\mathrm{L}}, \hat{\mathbf{E}}_i^{\mathrm{L}\dagger}|0\rangle_{\mathrm{L}}, \hat{\mathbf{B}}_i^{\mathrm{L}\dagger}|0\rangle_{\mathrm{L}}, \hat{\mathbf{E}}_i^{\mathrm{L}\dagger}\hat{\mathbf{B}}_j^{\mathrm{L}\dagger}|0\rangle_{\mathrm{L}}, \cdots\}, \tag{5.34}$$

$$\mathscr{H}_{\mathrm{R}} = \mathrm{Span}\{|0\rangle_{\mathrm{R}}, \hat{\mathbf{E}}_i^{\mathrm{R}\dagger}|0\rangle_{\mathrm{R}}, \hat{\mathbf{B}}_i^{\mathrm{R}\dagger}|0\rangle_{\mathrm{R}}, \hat{\mathbf{E}}_i^{\mathrm{R}\dagger}\hat{\mathbf{B}}_j^{\mathrm{R}\dagger}|0\rangle_{\mathrm{R}}, \cdots\}. \tag{5.35}$$

where the corresponding vacuum states $|0\rangle_{\mathrm{L}}$ and $|0\rangle_{\mathrm{R}}$ satisfy

$$\hat{\mathbf{E}}_i^{\mathrm{L}}|0\rangle_{\mathrm{L}} = \hat{\mathbf{B}}_i^{\mathrm{L}}|0\rangle_{\mathrm{L}} = \hat{\mathbf{E}}_i^{\mathrm{R}}|0\rangle_{\mathrm{R}} = \hat{\mathbf{B}}_i^{\mathrm{R}}|0\rangle_{\mathrm{R}} = 0. \tag{5.36}$$

The total Hilbert space is then

$$\mathscr{H}_{\mathrm{L}} \otimes \mathscr{H}_{\mathrm{R}} \tag{5.37}$$

Their normalized n-particle states are denoted as

$$|\hat{\mathbf{E}}_1^{\mathrm{L}}\rangle = \mathcal{N}\hat{\mathbf{E}}_1^{\mathrm{L}\dagger}|0\rangle_{\mathrm{L}} \tag{5.38}$$

where $\mathcal{N}$ is a normalization constant.

The effective state we need to evaluate the Rényi EE in LTA, is the one where we replace the field operator with the corresponding the LTA operator. For example, if we have inserted $(\mathbf{E}_1)^2$ in QFT, then the corresponding effective state is

$$|\psi^{\text{eff}}\rangle = \mathcal{N}\left(\hat{\mathbf{E}}_1\right)^2 |0\rangle_{\text{L}} \otimes |0\rangle_{\text{R}} \tag{5.39}$$

with a normalization constant $\mathcal{N}$. By using this LTA, we are able to reproduce the Rényi EE growth $\Delta S_{\mathcal{A}}^{(n)}$ for Lorentz invariant operator insertions, such as

$$\hat{\mathbf{F}}_{\mu\nu}\hat{\mathbf{F}}^{\mu\nu}, \hat{\mathbf{E}}^2 + \hat{\mathbf{B}}^2, \tag{5.40}$$

and the ones where the operators $\hat{\mathbf{E}}_2, \hat{\mathbf{E}}_3, \hat{\mathbf{B}}_2, \hat{\mathbf{B}}_3$ are mixed symmetrically as

$$\hat{\mathbf{E}}_2\hat{\mathbf{B}}_3 - \hat{\mathbf{E}}_3\hat{\mathbf{B}}_2, \tag{5.41}$$

which is the Poynting vector towards the entangling surface Σ.

We now propose the commutation relations for finite time. For the gauge theory case, there is no geometrical understanding like in scalar field yet.

We show here the explicit expression for 4 dimensional spacetime at finite time and correspondingly in the late time limit. In 4-dimensional spacetime:

$$\left[\hat{\mathbf{E}}_1^{\text{L}}, \hat{\mathbf{E}}_1^{\text{L}\dagger}\right] = \frac{(2t-\ell)\,(t+\ell)^2}{2t^3} \qquad \underset{t\to\infty}{\longrightarrow} 1 \tag{5.42}$$

$$\left[\hat{\mathbf{E}}_1^{\text{R}}, \hat{\mathbf{E}}_1^{\text{R}\dagger}\right] = \frac{(2t+\ell)\,(t-\ell)^2}{2t^3} \qquad \underset{t\to\infty}{\longrightarrow} 1 \tag{5.43}$$

$$\left[\hat{\mathbf{E}}_i^{\text{L}}, \hat{\mathbf{E}}_j^{\text{L}\dagger}\right] = \delta_{ij}\frac{4t^3+3\ell t^2+\ell^3}{4t^3} \qquad \underset{t\to\infty}{\longrightarrow} \delta_{ij} \tag{5.44}$$

$$\left[\hat{\mathbf{E}}_i^{\text{R}}, \hat{\mathbf{E}}_j^{\text{R}\dagger}\right] = \delta_{ij}\frac{4t^3-3\ell t^2-\ell^3}{4t^3} \qquad \underset{t\to\infty}{\longrightarrow} \delta_{ij} \tag{5.45}$$

$$\left[\hat{\mathbf{E}}_2^{\text{L}}, \hat{\mathbf{B}}_3^{\text{L}\dagger}\right] = \frac{3\,(t-\ell)\,(t+\ell)}{4t^2} \qquad \underset{t\to\infty}{\longrightarrow} \frac{3}{4} \tag{5.46}$$

$$\left[\hat{\mathbf{E}}_2^{\text{R}}, \hat{\mathbf{B}}_3^{\text{R}\dagger}\right] = -\frac{3\,(t-\ell)\,(t+\ell)}{4t^2} \qquad \underset{t\to\infty}{\longrightarrow} -\frac{3}{4} \tag{5.47}$$

$$\left[\hat{\mathbf{E}}_3^{\text{L}}, \hat{\mathbf{B}}_2^{\text{L}\dagger}\right] = -\frac{3\,(t-\ell)\,(t+\ell)}{4t^2} \qquad \underset{t\to\infty}{\longrightarrow} -\frac{3}{4} \tag{5.48}$$

$$\left[\hat{\mathbf{E}}_3^{\text{R}}, \hat{\mathbf{B}}_2^{\text{R}\dagger}\right] = \frac{3\,(t-\ell)\,(\ell+t)}{4t^2} \qquad \underset{t\to\infty}{\longrightarrow} \frac{3}{4} \tag{5.49}$$

where $i, j \in \{2, 3\}$. By using this LTA, we get the following effective density matrix $\rho_{\mathcal{A}}^{\text{eff}}$ for example:

$$E_1 \text{ or } E_2 : \begin{pmatrix} \frac{1}{2} & 0 \\ 0 & \frac{1}{2} \end{pmatrix} \tag{5.50}$$

$$F^2 : \frac{1}{192} \begin{pmatrix} 30 & & & & & & & & \\ & 30 & & & & & & & \\ & & 16 & & & & & & \\ & & & 16 & & & & & \\ & & & & 49 & & & & \\ & & & & & 49 & & & \\ & & & & & & 1 & & \\ & & & & & & & 1 & \end{pmatrix} \tag{5.51}$$

Let us conclude this section with some remarks. The Rényi EE growth $\Delta S_{\mathcal{A}}^{(n)}$ for locally excited states is invariant under the S-duality transformation $\mathbf{E}_i \to -\mathbf{B}_i$ and $\mathbf{B}_i \to \mathbf{E}_i$. Since the Rényi EE growth $\Delta S_{\mathcal{A}}^{(n)}$ reflects the electric-magnetic duality, the entropy for $\mathbf{B}_i$ is equal to that for $\mathbf{E}_i$. On the other hand, the Rényi EE growth $\Delta S_{\mathcal{A}}^{(n)}$ depends on the direction relative to the entangling surface Σ. The Rényi EE growth $\Delta S_{\mathcal{A}}^{(n)}$ for the fields vertical to the entangling surface Σ increases slower than those parallel to it. However, there are no differences of the Rényi EE growth $\Delta S_{\mathcal{A}}^{(n)}$ between inserting one electromagnetic field $\mathbf{E}_i$ or $\mathbf{B}_i$ and that of one scalar insertion in the late time limit $t \to \infty$.

We can find the difference in late time of Maxwell field and scalar field by considering the case for composite operators, namely the combinations of $\mathbf{E}_2, \mathbf{B}_3$ and $\mathbf{E}_3, \mathbf{B}_2$. This is encoded into the LTA and FTA as nonzero commutation relation in $\hat{\mathbf{E}}_2, \hat{\mathbf{B}}_3$ and $\hat{\mathbf{E}}_3, \hat{\mathbf{B}}_2$. These are corresponding to the combinations of electric and magnetic operators parallel to the entangling surface Σ.

Chapter 6

Conclusion

Quantum Entanglement is one of the properties at the heart of the quantum theory, and is an indispensable concept in modern physics. Though this property was realized from the very beginning of quantum theory, it has often been the source of controversial issues. Recently it is rediscovered to be related to the phenomena of hot research topics like black hole entropy and information loss, increasing its importance again.

In this thesis, we have discussed the Rényi EE growth which is the difference of Rényi entanglement entropy of a locally excited state compared to the one of the vacuum state. The *Late Time Algebra* is an algebra describing the Rényi entanglement entropy growth in the limit $t \to \infty$, and gives a quasi-particle picture to it. First we gave a method to define the commutation relation of the *Late Time Algebra* from the corresponding Quantum Field Theory in a systematical way. Then, we introduced the *Finite Time Algebra* by extending the *Late Time Algebra* to each time slice. This gives a quasi-particle picture at every time slice for the Rényi entanglement entropy growth in Quantum Field Theory.

We also presented the *Particle Propagating Model*, which is a new model for 4-dimensional free scalar field theory. It provides an intuitive understanding to

the Rényi entanglement entropy growth. In this model, the Rényi entanglement entropy growth is obtained as the Rényi entropy of a quasi-particle that propagates isotropically in space. The Rényi entanglement entropy growth is defined by the area ratio of the two surfaces into which the sphere is divided by the entangling surface, where the sphere is the position of particle propagating at the speed of light. Therefore, the Rényi entanglement entropy growth is a kind of measure for the degree of freedom of this quantum mechanical system.

The second topic we addressed in this thesis is about the Rényi entanglement entropy growth in gauge theory. There are still discussions on how to define the entanglement entropy for gauge theories, since a naïve definition leads it to be gauge dependent. However, the Rényi entanglement entropy growth in this thesis is defined uniquely without gauge dependence, as far as the assumption holds that the effect of gauge choice appears on the boundary as the boundary condition. We have also shown that the Rényi entanglement entropy growth in Maxwell theory respects the causality, as it is in the case for scalar field theory.

The late time algebra and finite time algebra show that Maxwell theory also admits a quasi-particle description. We can see that there is a different property in entanglement from that of a scalar field. The mixing of the operators associated to different directions in the algebras distinguishes the Maxwell fields from scalar fields.

The definition of entanglement entropy in gauge theory is a very subtle issue, and some modification is needed to make it compatible with gauge invariance. From our point of view, it would be very interesting to construct the particle propagating model for gauge theory and discuss the difference of time development of Rényi entanglement entropy from the scalar theory case. Our discussion presented in this thesis is free from this gauge invariance problem, and therefore it may shed some light on understanding the entanglement of gauge fields.

Acknowledgement

First, I would like to thank all colleagues in the E-lab at Nagoya University. The good environment, their support and stimulating discussions were helpful to finish this work. I thank my supervisor Tadakatsu Sakai for his support and for allowing me freely to pursue this project. Especially I would like to thank Masahiro Nozaki for his kindness and patience in the discussions about the subject of this thesis. The main results of this thesis are based on the works with him. I would like to thank Achim Kempf for his kindness and hospitality during my stay at University of Waterloo, and many encouraging advice I received from him. The incredible hospitality of Achim Kempf and Dushyantha Kempf made my stay at University of Waterloo very successful and wonderful, making me even enjoy the coldness of the winter in Canada for three months. I also want to thank Eduardo Martin-Martinez, not only for the valuable discussions, but also for let me join his group where I learned a lot. I would also like to thank Yasusada Nambu and Masahiro Hotta for valuable discussions and encouraging advice.

I would like to thank the Nagoya University Program for Leading Graduate Schools "Leadership Development Program for Space Exploration and Research" for the valuable experiences and financial support.

Appendix A

Examples of Scalar fields

A.1 Example of Scalar FTA

Here we demonstrate the FTA calculation to obtain the Rényi EE growth $\Delta S_{\mathcal{A}}^{(n)}$ for the insertion of $:\phi^k:$. The FTA given in the main part for 4 dimension is:

$$\begin{aligned}\left[\hat{\phi}^{\mathrm{L}}, \hat{\phi}^{\mathrm{L}\dagger}\right] &= \lim_{\epsilon\to 0} 32\pi^2\epsilon^2 G^{(n)}(\theta_1-\theta_2),\\ \left[\hat{\phi}^{\mathrm{R}}, \hat{\phi}^{\mathrm{R}\dagger}\right] &= \lim_{\epsilon\to 0} 32\pi^2\epsilon^2 G^{(n)}(\theta_1-\theta_2+2\pi),\end{aligned} \tag{A.1}$$

We also have the relation

$$\lim_{\epsilon\to 0}\epsilon^2 G^{(1)}(\theta_1-\theta_2) = \lim_{\epsilon\to 0}\epsilon^2\left(G^{(n)}(\theta_1-\theta_2)+G^{(n)}(\theta_1-\theta_2+2\pi)\right). \tag{A.2}$$

from the explicit calculation.

We evaluate the LTA for the locally excited state:

$$|\psi^{\mathrm{ex}}\rangle = \mathcal{N}:\phi^k(-t,-l,\mathbf{x}):|0\rangle \tag{A.3}$$

where $\mathcal{N}$ is a normalization constant, that is given by

$$\mathcal{N} = \frac{1}{k!(32\pi^2\epsilon^2)^k(G^{(n)}(\theta_1-\theta_2)+G^{(n)}(\theta_1-\theta_2+2\pi))^k}, \tag{A.4}$$

and $\mathbf{x}$ is the coordinate for the 2 and 3 direction. The effective reduced density matrix of this excited state is given by[1]

$$\rho_{\mathcal{A}}^{\text{eff}} = \text{tr}_{\text{L}}(\rho) = \sum_{s=0}^{k} \frac{{}_kC_s \left(G^{(n)}(\theta_1-\theta_2)\right)^{k-s} \left(G^{(n)}(\theta_1-\theta_2+2\pi)\right)^{s}}{\left(G^{(n)}(\theta_1-\theta_2)+G^{(n)}(\theta_1-\theta_2+2\pi)\right)^{k}} |s\rangle_{\text{RR}}\langle s|. \quad \text{(A.5)}$$

Then $S_{\mathcal{A}}^{(n)}$ for this density matrix in (A.5) is given by

$$\begin{aligned}\Delta S_{\mathcal{A}}^{(n)} &= \frac{1}{1-n}\log\left[\sum_{s=0}^{k}\left(\frac{{}_kC_s \left(G^{(n)}(\theta_1-\theta_2)\right)^{k-s} \left(G^{(n)}(\theta_1-\theta_2+2\pi)\right)^{s}}{\left(G^{(n)}(\theta_1-\theta_2)+G^{(n)}(\theta_1-\theta_2+2\pi)\right)^{k}}\right)^{n}\right] \quad \text{(A.6)}\\ &= \frac{1}{1-n}\log\left[\sum_{s=0}^{k}\left({}_kC_s (P_{\text{L}}(t))^{k-s}(P_{\text{R}}(t))^{s}\right)^{n}\right].\end{aligned}$$

where we use the identity in (A.2). The entropy in the late time limit is given by

$$\Delta S_{\mathcal{A}}^{(n)} = \frac{1}{1-n}\log\left[2^{-kn}\sum_{s=0}^{k}({}_kC_s)^{n}\right]. \quad \text{(A.7)}$$

These results in (A.6) and (A.7) are consistent with the results in the replica method[18, 19].

A.2 Example for PPM

Here, we give examples of calculations using the particle propagating model. We compute the Rényi EE growth $\Delta S_{\mathcal{A}}^{(n)}$ by using this model. Recall the assumptions of PPM:

- *One* local operator creates *one* quasi-particle.
- Quasi-particles created at the *same* point of spacetime *cannot be distinguished*.

Note that the spacetime is 4-dimensional and flat : $\mathcal{M} = \mathbb{R}^4$.

[1] ${}_kC_s$ is a binomial coefficient defined by ${}_kC_s := \frac{(k)!}{s!(k-s)!}$.

A.2.1 Example.1: Composite operator $\mathcal{O} =: \phi^k(-t, -\ell, \mathbf{x}) :$

We start with the example of a local operator $: \phi^k :$ located at $(x^0, x^1, x^2, x^3) = (-t, -\ell, 0, 0)$ acts on the ground state. Then in $t > \ell$, the s particles and $k - s$ particles are included in $\mathcal{A}$ and $\mathcal{B}$ with the probability ${}_kC_s \left(P_{\mathcal{A}}(t, \ell)\right)^{k-s} \left(P_{\mathcal{B}}(t, \ell)\right)^s$. Thus the probability distribution ρ is given by

$$\rho^{\text{PPM}} = \sum_{s=0}^{k} {}_kC_s \left(P_{\mathcal{A}}(t, \ell)\right)^{k-s} \left(P_{\mathcal{B}}(t, \ell)\right)^s |s; k-s\rangle\langle s; k-s|, \tag{A.8}$$

where $|l; k-l\rangle$ is the state where l and $k-l$ particles are included in $\mathcal{A}$ and $\mathcal{B}$, respectively. The Rényi EE $S^{(n)}$ of this reduced density matrix ρ^{PPM} (A.8) is consistent with the Rényi EE growth $\Delta S_{\mathcal{A}}^{(n)}$ in (A.6).

A.2.2 Example.2 : Two operators at different point in spacetime $\mathcal{O} = \phi(-T, -L, \mathbf{x}_1)\phi(-t, -\ell, \mathbf{x}_2)$

The second example is a state where two scalar fields are acting at different points in spacetime. The corresponding excited state $|\psi^{\text{ex}}\rangle$ is with the operator insertion $\mathcal{O} = \phi(-T, -L, \mathbf{x}_1)\phi(-t, -\ell, \mathbf{x}_2)$,

$$|\psi^{\text{ex}}\rangle = \mathcal{N}\phi(-T, -L, \mathbf{x}_1)\phi(-t, -\ell, \mathbf{x}_2)|0\rangle, \tag{A.9}$$

where $\ell, L, t, T > 0$, $\mathcal{N}$ is a normalization constant, and $\mathbf{x}_1, \mathbf{x}_2$ are the coordinates for $2, 3$ direction which are constants. Since we distinguish the particles created at different points in spacetime, the density matrix ρ^{PPM} at $t = 0$ is defined by

$$\begin{aligned}
\rho^{\text{PPM}} &= \sum_{a,b;c,d} P_{a,c}\tilde{P}_{b,d}|a, b; c, d\rangle\langle a, b; c, d| \\
&= P_{1,0}\tilde{P}_{1,0}|1, 1; 0, 0\rangle\langle 1, 1; 0, 0| + P_{0,1}\tilde{P}_{1,0}|0, 1; 1, 0\rangle\langle 0, 1; 1, 0| \\
&+ P_{0,1}\tilde{P}_{0,1}|1, 0; 0, 1\rangle\langle 1, 0; 0, 1| + P_{0,1}\tilde{P}_{0,1}|0, 0; 1, 1\rangle\langle 0, 0; 1, 1|,
\end{aligned} \tag{A.10}$$

where $|a, b; c, d\rangle$ is the state where a (b) and c (d) particles created by $\phi(-T, -L, \mathbf{x}_1)$ $(\phi(-t, -\ell, \mathbf{x}_2))$ are included in $\mathcal{A}$ and $\mathcal{B}$, respectively. $P_{a,b}$ and $\tilde{P}_{c,d}$ is the probability

for each quasi-particle created at $(-T, -L, \mathbf{x}_1)$ and $(-t, -\ell, \mathbf{x}_2)$, respectively. They are given by

$$P_{1,0} = \begin{cases} 0 & T < L \\ \frac{(T-L)}{2T} & T \geqq L \end{cases}, \qquad P_{0,1} = \begin{cases} 1 & T < L \\ \frac{(T+L)}{2T} & T \geqq L \end{cases}, \\ \tilde{P}_{1,0} = \begin{cases} 0 & t < \ell \\ \frac{(t-\ell)}{2(t)} & t \geqq \ell \end{cases}, \qquad \tilde{P}_{0,1} = \begin{cases} 1 & t < \ell \\ \frac{(t+\ell)}{2(t)} & t \geqq \ell \end{cases}. \tag{A.11}$$

Thus, when we compute the Rényi EE $S^{(n),\text{PPM}}$ of the density matrix (A.10), we obtain

$$S^{(n>1),\text{PPM}} = \frac{1}{1-n} \log \left[\left(P_{1,0}\tilde{P}_{1,0} \right)^n + \left(P_{0,1}\tilde{P}_{1,0} \right)^n + \left(P_{1,0}\tilde{P}_{0,1} \right)^n + \left(P_{0,1}\tilde{P}_{0,1} \right)^n \right]. \tag{A.12}$$

In the limit $n \to 1$ where we recover the EE, we get

$$\begin{aligned} \lim_{n\to 1} S^{((n)),\text{PPM}} = &- \left(P_{1,0}\tilde{P}_{1,0} \right) \log \left(P_{1,0}\tilde{P}_{1,0} \right) - \left(P_{0,1}\tilde{P}_{1,0} \right) \log \left(P_{0,1}\tilde{P}_{1,0} \right) \\ &- \left(P_{1,0}\tilde{P}_{0,1} \right) \log \left(P_{1,0}\tilde{P}_{0,1} \right) - \left(P_{0,1}\tilde{P}_{0,1} \right) \log \left(P_{0,1}\tilde{P}_{0,1} \right). \end{aligned} \tag{A.13}$$

It is straight forward to check that in the late time limit, this Rényi EE $S^{(n),\text{PPM}}$ converges and we get $S^{((n\geq 1)),\text{PPM}} = \log 4$. This is consistent with the result in [19].

A.2.3 Example.3: Space Decomposition with a Finite Interval

In the third example, we insert one scalar operator at $(-t, -\ell)$ where $t > 0, \ell > 0$. This is the same as the first example, however we change the definition of subregions $\mathcal{A}$ and $\mathcal{B}$ in this example. The subregions $\mathcal{A}$ and $\mathcal{B}$ are defined as

$$\begin{aligned} \mathcal{A} &= \{ p \in \mathcal{M}_0 | 0 \leq x^1(p) < L \} \\ \mathcal{B} &= \mathcal{A}^c, \end{aligned} \tag{A.14}$$

where $\mathcal{A}^c$ is the complement of $\mathcal{A}$ in $\mathcal{M}_0$. We denote the probability that the created quasi-particle is included in the subregion $\mathcal{A}$, $\mathcal{B}$ as $P_{\mathcal{A}}(t)$, $P_{\mathcal{B}}(t)$, respectively. They are given by

$$P_{\mathcal{A}}(t) = \begin{cases} 0 & 0 \leqq t < \ell \\ \frac{t-\ell}{2t} & 0 < \ell \leqq t < L+\ell\,, \\ \frac{L}{2t} & L+\ell+\ell \leq t \end{cases} \quad P_{\mathcal{B}}(t) = \begin{cases} 1 & 0 \leqq t < \ell \\ \frac{t+\ell}{2t} & 0 < \ell \leqq t < L+\ell\,. \\ \frac{2t-L}{2t} & L+\ell \leqq t \end{cases} \tag{A.15}$$

The probability $P_{\mathcal{A}}(t)$ and $P_{\mathcal{B}}$ corresponds to the area of sphere $\mathcal{K}$, that is included in each subregion $\mathcal{A}$ and $\mathcal{B}$, respectively. The Rényi EE $S^{(n),\mathrm{PPM}}$ and EE is given by

$$S^{(n),\mathrm{PPM}} = \begin{cases} 0 & 0 < t < \ell \\ \frac{1}{1-n}\log\left[(\frac{t-\ell}{2t})^n + (\frac{t+\ell}{2t})^n\right] & 0 < \ell \leqq t < L\,, \\ \frac{1}{1-n}\log\left[(\frac{2t-L}{2t})^n + (\frac{L}{2t})^n\right] & L \leqq t \end{cases}$$

$$\lim_{n\to 1} S^{(n),\mathrm{PPM}} = S^{(1),\mathrm{PPM}} = \begin{cases} 0 & 0 < t < \ell \\ -\left(\frac{t-\ell}{2t}\right)\log\left(\frac{t-\ell}{2t}\right) - \left(\frac{t+\ell}{2t}\right)\log\left(\frac{t+\ell}{2t}\right) & 0 < \ell \leqq t < L+\ell\,. \\ -\left(\frac{2t-L}{2t}\right)\log\left(\frac{2t-L}{2t}\right) - \left(\frac{L}{2t}\right)\log\left(\frac{L}{2t}\right) & L+\ell \leqq t \end{cases} \tag{A.16}$$

The plot of EE $S^{(1),\mathrm{PPM}}$ shows an increases after $t = \ell$ and decreases after $t = L + \ell$ (Fig.A.1) before it reaches the value $\log 2$. This is because the probability $P_{\mathcal{A}}(t)$ increases in $\ell < t < L + \ell$ but it does not reach the value $\frac{1}{2}$ and starts to decrease. The EE does not reach the maximally entangled state that we obtained in the case of two infinite subsystems and vanishes at the late time.

A.2.4 Example.4: Infinite Subsystems

In the forth example, we divide the space into infinite subregions in an more complicated way than that one discussed in the main part. We consider two patterns to

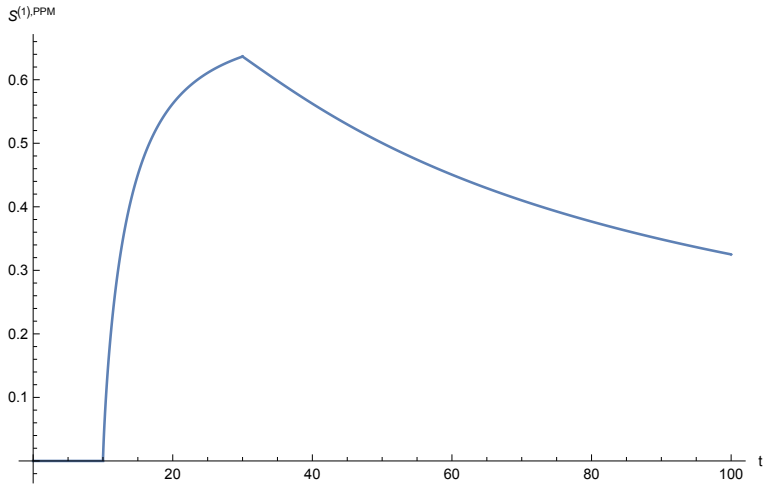

Figure A.1: The plot of EE $S^{(1),\mathrm{PPM}}$.The horizontal axis is t, and the vertical axis is S. The values of $(\ell, L) = (10, 20)$.

divide the space into two infinite subregions, $\mathcal{A}_1$, $\mathcal{B}_1$ and $\mathcal{A}_2$, $\mathcal{B}_2$. They are defined as follows,

$$\begin{aligned} \mathcal{A}_1 &= \{x_1 \geq l, x_2 \geq 0\}, \\ \mathcal{B}_1 &= \mathcal{A}_1^c, \\ \mathcal{A}_2 &= \{x_1 \geq l, x_2 \geq 0, x_3 \geq 0\}, \\ \mathcal{B}_2 &= \mathcal{A}_2^c, \end{aligned} \tag{A.17}$$

where the complement is defined in $\mathcal{M}_0$. The local operator is ϕ and located at $(-t, -\ell)$. The density matrix for each case ρ_i^{PPM} is given by

$$\rho_i^{\mathrm{PPM}} := P_{\mathcal{B}_i}(t)|0;1\rangle\langle 0;1| + P_{\mathcal{A}_i}(t)|1;0\rangle\langle 1;0|, (i = 1 \sim 2) \tag{A.18}$$

where $i = 1, 2$, the probabilities are given by

$$\begin{aligned} P_{\mathcal{A}_1}(t) &= \frac{1}{4}\left(1 - \frac{\ell}{t}\right), \quad P_{\mathcal{B}_1}(t) = \frac{1}{4}\left(3 + \frac{\ell}{t}\right), \\ P_{\mathcal{A}_2}(t) &= \frac{1}{8}\left(1 - \frac{\ell}{t}\right), \quad P_{\mathcal{B}_2}(t) = \frac{1}{8}\left(7 + \frac{\ell}{t}\right), \end{aligned} \tag{A.19}$$

and the state $|s; k-s\rangle$ is describing the state where s and $k-s$ particles are included in $\mathcal{A}_i$ and $\mathcal{B}_i$ respectively.

As in the other cases, their entropy in $t \leqq \ell$ vanishes. Their Rényi Entropy $S^{(n),\mathrm{PPM}}$ in $t > \ell$ is

$$\begin{aligned}
S^{(n),\mathrm{PPM}}(\rho_1) &= \begin{cases} \frac{1}{1-n}\log\left[\left(\frac{1}{4}\left(1-\frac{\ell}{t}\right)\right)^n + \left(\frac{1}{4}\left(3+\frac{\ell}{t}\right)\right)^n\right] & n \geqq 2, \\ -\frac{1}{4}\left(1-\frac{\ell}{t}\right)\log\left[\frac{1}{4}\left(1-\frac{\ell}{t}\right)\right] - \frac{1}{4}\left(3+\frac{\ell}{t}\right)\log\left[\frac{1}{4}\left(3+\frac{\ell}{t}\right)\right] & n = 1, \end{cases} \\
S^{(n),\mathrm{PPM}}(\rho_2) &= \begin{cases} \frac{1}{1-n}\log\left[\left(\frac{1}{8}\left(1-\frac{\ell}{t}\right)\right)^n + \left(\frac{1}{8}\left(7+\frac{\ell}{t}\right)\right)^n\right] & n \geqq 2, \\ -\frac{1}{8}\left(1-\frac{\ell}{t}\right)\log\left[\frac{1}{8}\left(1-\frac{\ell}{t}\right)\right] - \frac{1}{8}\left(7+\frac{\ell}{t}\right)\log\left[\frac{1}{8}\left(7+\frac{\ell}{t}\right)\right] & n = 1. \end{cases}
\end{aligned} \tag{A.20}$$

The Rényi Entropy $S^{(n),\mathrm{PPM}}$ in the late time limit $t \to \infty$ is finite.

$$\begin{aligned}
S^{(n),\mathrm{PPM}}(\rho_1) &= \begin{cases} \frac{1}{1-n}\log\left[\left(\frac{1}{4}\right)^n + \left(\frac{3}{4}\right)^n\right] & n \geqq 2, \\ -\frac{1}{4}\log\left[\frac{1}{4}\right] - \frac{3}{4}\log\left[\frac{3}{4}\right] & n = 1, \end{cases} \\
S^{(n),\mathrm{PPM}}(\rho_2) &= \begin{cases} \frac{1}{1-n}\log\left[\left(\frac{1}{8}\right)^n + \left(\frac{7}{8}\right)^n\right] & n \geqq 2, \\ -\frac{1}{8}\log\left[\frac{1}{8}\right] - \frac{7}{8}\log\left[\frac{7}{8}\right] & n = 1. \end{cases}
\end{aligned} \tag{A.21}$$

This is due to the fact that the particle created by local operator ϕ has non-zero probability to be found in the subregions $\mathcal{A}_{1,2}$ in the late time limit. For the $n = 1$ case where we obtain the EE, they are both smaller than the entropy for an EPR state $\log 2$, which was the case discussed in the main text.

Appendix B

Rényi EE Growth of Maxwell theory

We will give here the leading term in ϵ dependence of the Green's functions, and examples of the Rényi EE growth $\Delta S_{\mathcal{A}}^{(n)}$ for Maxwell fields.

B.1 Green's Functions

The leading term in ϵ dependence for each fields in 4 and 6-dimensional spacetime are as follows.

In 4 space time dimension, we recall that the operators $\mathbf{E}_i, \mathbf{B}_i$ are defined in Euclidean space as

$$\mathbf{E}_i = -iF_{0i}, \mathbf{B}_i = -\varepsilon_{ijk}F^{jk} \tag{B.1}$$

where $i, j, k \in \{1, 2, 3\}$, and ε_{ijk} is the completely antisymmetric tensor. The ana-

lytic continued Green's functions on manifold $\mathcal{M}^{(n)}$ are defined by

$$\begin{aligned}
\langle \mathbf{E}_1(\theta)\mathbf{E}_1(\theta')\rangle_{\mathcal{M}^{(n)}} &= F^{(n)}_{E1E1}(\theta-\theta'),\\
\langle \mathbf{E}_2(\theta)\mathbf{E}_2(\theta')\rangle_{\mathcal{M}^{(n)}} &= \langle \mathbf{E}_3(\theta)\mathbf{E}_3(\theta')\rangle_{\mathcal{M}^{(n)}} = F^{(n)}_{E2E2}(\theta-\theta'),\\
\langle \mathbf{B}_1(\theta)\mathbf{B}_1(\theta')\rangle_{\mathcal{M}^{(n)}} &= F^{(n)}_{B1B1}(\theta-\theta'),\\
\langle \mathbf{B}_2(\theta)\mathbf{B}_2(\theta')\rangle_{\mathcal{M}^{(n)}} &= \langle \mathbf{B}_3(\theta)\mathbf{B}_3(\theta')\rangle_{\mathcal{M}^{(n)}} = F^{(n)}_{B2B2}(\theta-\theta'),\\
\langle \mathbf{E}_2(\theta)\mathbf{B}_3(\theta')\rangle_{\mathcal{M}^{(n)}} &= F^{(n)}_{E2B3}(\theta-\theta'),\\
\langle \mathbf{B}_3(\theta)\mathbf{E}_2(\theta')\rangle_{\mathcal{M}^{(n)}} &= F^{(n)}_{B3E2}(\theta-\theta'),\\
\langle \mathbf{E}_3(\theta)\mathbf{B}_2(\theta')\rangle_{\mathcal{M}^{(n)}} &= F^{(n)}_{E3B2}(\theta-\theta'),\\
\langle \mathbf{B}_2(\theta)\mathbf{E}_3(\theta')\rangle_{\mathcal{M}^{(n)}} &= F^{(n)}_{B2E3}(\theta-\theta').
\end{aligned} \tag{B.2}$$

If the limit $\epsilon \to 0$ is taken, their leading terms for $n = 1$ are given by

$$\begin{aligned}
F^{(1)}_{E1E1}(\theta_1-\theta_2) &\sim \frac{1}{16\pi^2\epsilon^4},\\
F^{(1)}_{E2E2}(\theta_1-\theta_2) &\sim \frac{1}{16\pi^2\epsilon^4},\\
F^{(1)}_{B1B1}(\theta_1-\theta_2) &\sim \frac{1}{16\pi^2\epsilon^4},\\
F^{(1)}_{B2B2}(\theta_1-\theta_2) &\sim \frac{1}{16\pi^2\epsilon^4}.
\end{aligned} \tag{B.3}$$

The leading terms in the limit $\epsilon \to 0$ of two-point functions are more complicated in the case $n \geqq 2$. If $0 < t < l$, they are the same as given in (B.3). If $0 < l \leq t$,

they are given by

$$
\begin{aligned}
F^{(n)}_{E1E1}(\theta_1-\theta_2) &= F^{(n)}_{E1E1}(\theta_2-\theta_1) \sim -\frac{(l-2t)(l+t)^2}{64\pi^2 t^3\epsilon^4},\\
F^{(n)}_{E2E2}(\theta_1-\theta_2) &= F^{(n)}_{E2E2}(\theta_2-\theta_1) \sim \frac{l^3+3lt^2+4t^3}{128\pi^2 t^3\epsilon^4},\\
F^{(n)}_{B1B1}(\theta_1-\theta_2) &= F^{(n)}_{B1B1}(\theta_2-\theta_1) \sim -\frac{(l-2t)(l+t)^2}{64\pi^2 t^3\epsilon^4},\\
F^{(n)}_{B2B2}(\theta_1-\theta_2) &= F^{(n)}_{B2B2}(\theta_2-\theta_1) \sim \frac{l^3+3lt^2+4t^3}{128\pi^2 t^3\epsilon^4},\\
F^{(n)}_{E2B3}(\theta_1-\theta_2) &= F^{(n)}_{E2B3}(\theta_2-\theta_1) \sim \frac{3(t-l)(l+t)}{128\pi^2 t^2\epsilon^4},\\
F^{(n)}_{B3E2}(\theta_1-\theta_2) &= F^{(n)}_{B3E2}(\theta_2-\theta_1) \sim \frac{3(t-l)(l+t)}{128\pi^2 t^2\epsilon^4},\\
F^{(n)}_{E3B2}(\theta_1-\theta_2) &= F^{(n)}_{E3B2}(\theta_2-\theta_1) \sim \frac{3(l-t)(l+t)}{128\pi^2 t^2\epsilon^4},\\
F^{(n)}_{B2E3}(\theta_1-\theta_2) &= F^{(n)}_{B2E3}(\theta_2-\theta_1) \sim \frac{3(l-t)(l+t)}{128\pi^2 t^2\epsilon^4},
\end{aligned}
\tag{B.4}
$$

and

$$
\begin{aligned}
&F_{E1E1}(\theta_1-\theta_2+2\pi)=F_{E1E1}(\theta_2-\theta_1-2\pi)\\
&=F_{E1E1}(\theta_1-\theta_2-2(n-1)\pi)=F_{E1E1}(\theta_2-\theta_1+2(n-1)\pi)\sim\frac{(l-t)^2(l+2t)}{64\pi^2t^3\epsilon^4},\\
&F_{E2E2}(\theta_1-\theta_2+2\pi)=F_{E2E2}(\theta_2-\theta_1-2\pi)\\
&=F_{E2E2}(\theta_1-\theta_2-2(n-1)\pi)=F_{E2E2}(\theta_2-\theta_1+2(n-1)\pi)\sim-\frac{l^3+3lt^2-4t^3}{128\pi^2t^3\epsilon^4},\\
&F_{B1B1}(\theta_1-\theta_2+2\pi)=F_{B1B1}(\theta_2-\theta_1-2\pi)\\
&=F_{B1B1}(\theta_1-\theta_2-2(n-1)\pi)=F_{B1B1}(\theta_2-\theta_1+2(n-1)\pi)\sim\frac{(l-t)^2(l+2t)}{64\pi^2t^3\epsilon^4},\\
&F_{B2B2}(\theta_1-\theta_2+2\pi)=F^{(n,l)}_{B2B2}(\theta_2-\theta_1-2\pi)\\
&=F_{B2B2}(\theta_1-\theta_2-2(n-1)\pi)=F^{(n,l)}_{B2B2}(\theta_2-\theta_1+2(n-1)\pi)\sim-\frac{l^3+3lt^2-4t^3}{128\pi^2t^3\epsilon^4},\\
&F_{E2B3}(\theta_1-\theta_2+2\pi)=F_{E2B3}(\theta_2-\theta_1-2\pi)\\
&=F_{E2B3}(\theta_1-\theta_2-2(n-1)\pi)=F_{E2B3}(\theta_2-\theta_1+2(n-1)\pi)\sim\frac{3(l-t)(l+t)}{128\pi^2t^2\epsilon^4},\\
&F_{B3E2}(\theta_1-\theta_2+2\pi)=F_{B3E2}(\theta_2-\theta_1-2\pi)\\
&=F_{B3E2}(\theta_1-\theta_2-2(n-1)\pi)=F_{B3E2}(\theta_2-\theta_1+2(n-1)\pi)\sim\frac{3(l-t)(l+t)}{128\pi^2t^2\epsilon^4},\\
&F_{E3B2}(\theta_1-\theta_2+2\pi)=F_{E3B2}(\theta_2-\theta_1-2\pi)\\
&=F_{E3B2}(\theta_1-\theta_2-2(n-1)\pi)=F_{E3B2}(\theta_2-\theta_1+2(n-1)\pi)\sim\frac{3(t-l)(l+t)}{128\pi^2t^2\epsilon^4},\\
&F_{B2E3}(\theta_1-\theta_2+2\pi)=F_{B2E3}(\theta_2-\theta_1-2\pi)\\
&=F_{B2E3}(\theta_1-\theta_2-2(n-1)\pi)=F_{B2E3}(\theta_2-\theta_1+2(n-1)\pi)\sim\frac{3(t-l)(l+t)}{128\pi^2t^2\epsilon^4}.
\end{aligned}
\tag{B.5}
$$

The ϵ dependence of the other propagators are of order $O(\epsilon^{-3})$, therefore they do not give an effect to the Rényi EE growth.

In the case of 6 spacetime dimensions, we denote the analytic continued Green's functions on $\mathcal{M}^{(n)}$ as

$$
\langle F_{ij}(\theta)F_{lm}(\theta')\rangle_{\mathcal{M}^{(n)}}=F^{(n)}_{F_{ij}F_{lm}}(\theta-\theta'). \tag{B.6}
$$

In the $\epsilon \to 0$ limit, their leading terms are as follows.

For the case of $n = 1$ in $t > 0$,

$$\begin{aligned} F^{(1)}_{F_{0i}F_{0i}}(\theta_1 - \theta_2) &\sim \frac{1}{16\pi^3\epsilon^6}, \\ F^{(1)}_{F_{ij}F_{ij}}(\theta_1 - \theta_2) &\sim \frac{1}{32\pi^3\epsilon^6} \ (i, j \neq 0). \end{aligned} \tag{B.7}$$

For the case of $n \geqq 2$, if $l > t > 0$ they are the same as in (B.7). In $t \geq l$, they are as follows, with $i, j = 2, 3, 4, 5$ and $i \neq j$:

$$\begin{aligned} F^{(n)}_{F_{01}F_{01}}(\theta_1 - \theta_2) &\sim \frac{1}{256\pi^3}\frac{(t+l)^3(3l^2 - 9lt + 8t^2)}{t^5\epsilon^6}, \\ F^{(n)}_{F_{01}F_{01}}(\theta_1 - \theta_2 + 2\pi) &\sim \frac{1}{256\pi^3}\frac{(t-l)^3(3l^2 + 9lt + 8t^2)}{t^5\epsilon^6}, \\ F^{(n)}_{F_{0i}F_{0i}}(\theta_1 - \theta_2) &\sim \frac{1}{1024\pi^3}\frac{(l+t)^2(32t^3 - 19lt^2 + 6l^2t - 3l^3)}{t^5\epsilon^6}, \\ F^{(n)}_{F_{0i}F_{0i}}(\theta_1 - \theta_2 + 2\pi) &\sim \frac{1}{1024\pi^3}\frac{32t^5 - 45lt^4 + 10l^3t^2 + 3l^5}{t^5\epsilon^6}, \\ F^{(n)}_{F_{1i}F_{1i}}(\theta_1 - \theta_2) &\sim \frac{1}{1024\pi^3}\frac{16t^5 + 15lt^4 + 10l^3t^2 - 9l^5}{t^5\epsilon^6}, \\ F^{(n)}_{F_{1i}F_{1i}}(\theta_1 - \theta_2 + 2\pi) &\sim \frac{1}{1024\pi^3}\frac{16t^5 - 15t^4l - 10t^2l^3 + 9l^5}{t^5\epsilon^6}, \\ F^{(n)}_{F_{ij}F_{ij}}(\theta_1 - \theta_2) &\sim \frac{1}{512\pi^3}\frac{(t+l)^3(3l^2 - 9lt + 8t^2)}{t^5\epsilon^6}, \\ F^{(n)}_{F_{ij}F_{ij}}(\theta_1 - \theta_2 + 2\pi) &\sim \frac{1}{512\pi^3}\frac{(t-l)^3(8t^2 + 9lt + 3l^2)}{t^5\epsilon^6}, \\ F^{(n)}_{F_{0i}F_{1i}}(\theta_1 - \theta_2) = F^{(n)}_{F_{1i}F_{0i}}(\theta_1 - \theta_2) &\sim \frac{15}{1024\pi^3}\frac{(t^2 - l^2)^2}{t^4\epsilon^6}, \\ F^{(n)}_{F_{0i}F_{1i}}(\theta_1 - \theta_2 + 2\pi) = F^{(n)}_{F_{1i}F_{0i}}(\theta_1 - \theta_2 + 2\pi) &\sim -\frac{15}{1024\pi^3}\frac{(t^2 - l^2)^2}{t^4\epsilon^6}. \end{aligned} \tag{B.8}$$

They have the property $F^{(n)}_{IJ}(\theta) = F^{(n)}_{IJ}(-\theta)$, and due to the periodicity of the n-sheeted Riemann surface, they all satisfy $F^{(n)}_{IJ}(\theta) = F^{(n)}_{IJ}(\theta \pm 2\pi n)$. The ϵ dependence of the other propagators are of order $O(\epsilon^{-5})$, therefore they do not give an effect to the Rényi EE growth.

$\mathcal{O}$	$\Delta S_{\mathcal{A}}^{(n)}$
E_1 or B_1	$\frac{1}{1-n}\log\left(\left(-\frac{(\ell+t)^2(\ell-2t)}{4t^3}\right)^n+\left(\frac{(t-\ell)^2(\ell+2t)}{4t^3}\right)^n\right)$
$E_{2,3}$ or $B_{2,3}$	$\frac{1}{1-n}\log\left(\left(\frac{-\ell^3-3\ell t^2+4t^3}{8t^3}\right)^n+\left(\frac{\ell^3+3\ell t^2+4t^3}{8t^3}\right)^n\right)$

Table B.1: $\Delta S_{\mathcal{A}}^{(n)}[\mathcal{O}]$ in the region $0 < l \leq t$

They are related as,

$$\begin{aligned}
&F^{(n)}_{F_{ij}F_{ij}}(\theta_1-\theta_2)+F^{(n)}_{F_{ij}F_{ij}}(\theta_1-\theta_2+2\pi)=F^{(1)}_{F_{ij}F_{ij}}(\theta_1-\theta_2),\\
&F^{(n)}_{F_{0i}F_{1i}}(\theta_1-\theta_2)+F^{(n)}_{F_{0i}F_{1i}}(\theta_1-\theta_2+2\pi)=0,\\
&F^{(n)}_{F_{1i}F_{0i}}(\theta_1-\theta_2)+F^{(n)}_{F_{1i}F_{0i}}(\theta_1-\theta_2+2\pi)=0,
\end{aligned} \tag{B.9}$$

where $n \geq 2$, $i, j = 2, 3, 4, 5$.

B.2 Examples of Rényi EE Growth in 4 Dimension

In the following sections, we give explicit examples of Rényi EE growth for Maxwell theory in 4 spacetime dimensions.

B.2.1 Single Operator Excitation

We start with the case of excitation generated by single operator $\mathbf{E}_i$ or $\mathbf{B}_j$. This is the easiest and simplest gauge invariant case of excitation. The result for excitations by inserting $\mathbf{E}_i$ or $\mathbf{B}_j$ is summarized in table B.1.

Due to the ϵ dependence of propagators, only the next neighbours' propagators contribute to the Rényi EE growth $\Delta S_{\mathcal{A}}^{(n)}$. Therefore, we have only two patterns of diagrams to evaluate Rényi EE growth $\Delta S_{\mathcal{A}}^{(n)}$ for integer $n \geqq 2$. This can be seen in the resulting function, where we have only two terms with the power of n.

The Rényi EE growth $\Delta S_{\mathcal{A}}^{(n)}$ that is summarized in the table B.1 is plotted in figure B.1. The vertical axis is $\Delta S_{\mathcal{A}}^{(2)}$, and the horizontal axis is t/ℓ. We can see that, the Rényi EE growth $\Delta S_{\mathcal{A}}^{(2)}$ is zero until the point $t/\ell = 1$. Then it starts to increase and approaches a certain value in both cases, $\mathbf{E}_1(\mathbf{B}_1)$ or $\mathbf{E}_{2,3}(\mathbf{B}_{2,3})$. The late time limit ($t/\ell \to \infty$) of Rényi EE growth $\Delta S_{\mathcal{A}}^{(n)}$ gives

$$\begin{aligned} \Delta S_{\mathcal{A}}^{(n)}[\mathbf{E}_1] = \Delta S_{\mathcal{A}}^{(n)}[\mathbf{B}_1] = & -\tfrac{1}{n-1}\log\left(\tfrac{1}{2}\right)^{n-1} = \log 2, \\ \Delta S_{\mathcal{A}}^{(n)}[\mathbf{E}_{2,3}] = \Delta S_{\mathcal{A}}^{(n)}[\mathbf{B}_{2,3}] = & -\tfrac{1}{n-1}\log\left(\tfrac{1}{2}\right)^{n-1} = \log 2. \end{aligned} \tag{B.10}$$

Thus, the limit $t/\ell \to \infty$ in Fig B.1 agrees in both cases, and they are $\log 2$. Equation (B.10) also shows that the late time limit ($t/\ell \to \infty$) of the EE $\Delta S_{\mathcal{A}}^{(1)}$ is

$$\Delta S_{\mathcal{A}}^{(1)} = \log 2 \tag{B.11}$$

for these cases.

The time dependence around $t \sim \ell$ is also interesting as refered to in the main text. As in figure B.1, the Rényi EE growth $\Delta S_{\mathcal{A}}^{(n)}$ of excitation with $\mathbf{E}_{2,3}$ or $\mathbf{B}_{2,3}$ increases faster then the excitation with $\mathbf{E}_1$ or $\mathbf{B}_2$. The behaviour of Rényi EE growth $\Delta S_{\mathcal{A}}^{(n)}$ around $t/\ell = 1$ (for $n \geqq 2$) is as follows,

$$\begin{aligned} \Delta S_{\mathcal{A}}^{(n)}[\mathbf{E}_1] = \Delta S_{\mathcal{A}}^{(n)}[\mathbf{B}_1] \sim & \ \tfrac{n}{n-1}\tfrac{3}{4}\left(\tfrac{t}{\ell}-1\right)^2, \\ \Delta S_{\mathcal{A}}^{(n)}[\mathbf{E}_{2,3}] = \Delta S_{\mathcal{A}}^{(n)}[\mathbf{B}_{2,3}] \sim & \ \tfrac{n}{n-1}\tfrac{3}{4}\left(\tfrac{t}{\ell}-1\right), \end{aligned} \tag{B.12}$$

where we omit the higher ϵ dependences. The physical understanding is explained in the main text.

Note that the result respects the electric-magnetic duality, which is the replacement of $\mathbf{E}_i \to -\mathbf{B}_i$ and $\mathbf{B}_i \to \mathbf{E}_i$.

B.2.2 Composite Operators

Here we show the time dependence of the Rényi EE growth $\Delta S_{\mathcal{A}}^{(n)}$ in composite operator case. First, we will give the case of combinations,

$$\mathbf{E}_i\mathbf{E}_i, \mathbf{E}_i\mathbf{E}_j, \mathbf{B}_i\mathbf{B}_i, \mathbf{B}_i\mathbf{B}_j, \mathbf{E}_i\mathbf{B}_i, \mathbf{E}_i\mathbf{B}_j \tag{B.13}$$

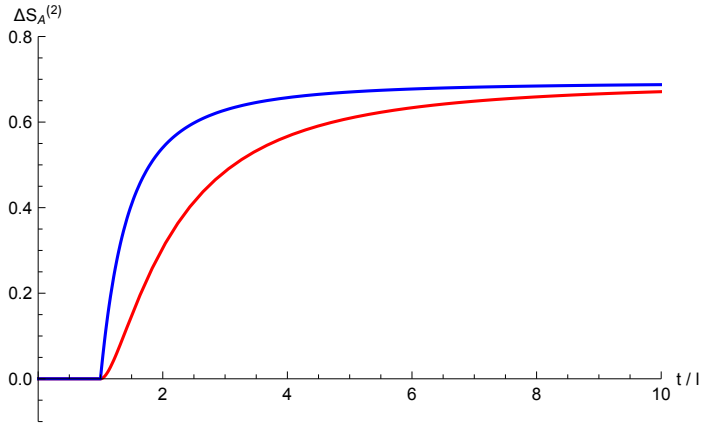

Figure B.1: The time evolution of the Rényi EE growth $\Delta S_{\mathcal{A}}^{(2)}$ for $\mathbf{E}_1(\mathbf{B}_1)$ and $\mathbf{E}_{2,3}(\mathbf{B}_{2,3})$. The horizontal and vertical axes correspond to the time t/l and Rényi EE growth $\Delta S_{\mathcal{A}}^{(2)}$, respectively. The lower line and upper line corresponds to the Rényi EE growth $\Delta S_{\mathcal{A}}^{(2)}$ for the excitation with field operator $\mathbf{E}_1(\mathbf{B}_1)$ and $\mathbf{E}_{2,3}(\mathbf{B}_{2,3})$, respectively.

where $i \neq j$.[1] In this case, we get a higher value for the Rényi EE growth $\Delta S_{\mathcal{A}}^{(n)}$ in the late lime limit $t \to \infty$ than in the case of a single operator, and their value in the limit is different.

The result is summarized in table B.2 and B.3. In all cases case except for $\mathbf{E}_2\mathbf{B}_3$ and $\mathbf{B}_2\mathbf{E}_3$, $\Delta S_{\mathcal{A}}^{(n)}$ is given in the form

$$\Delta S_{\mathcal{A}}^{(n)} = -\frac{1}{n-1} \log \left[\frac{N_1 + N_2 + N_3}{D_1} \right], \tag{B.14}$$

where N_i, $i = \{1, 2, 3\}$ is given in the table B.2, and the functions f_1, f_2, f_3, f_4 in the table are

$$\begin{aligned} f_1 &= -\frac{(\ell - 2t)(\ell + t)^2}{64t^3}, \\ f_2 &= \frac{(\ell + 2t)(\ell - t)^2}{64t^3}, \\ f_3 &= \frac{\ell^3 + 3\ell t^2 + 4t^3}{128t^3}, \\ f_4 &= \frac{-\ell^3 - 3\ell t^2 + 4t^3}{128t^3}. \end{aligned} \tag{B.15}$$

[1] In the expression (B.13), no sum is taken over the repeated indexes.

$\mathcal{O}$	D_1	N_1	N_2	N_3
$\mathbf{E}_1^2$ or $\mathbf{B}_1^2$	$\left(2\left(\frac{1}{16}\right)^2\right)^n$	$\left(2\left(f_1\right)^2\right)^n$	$\left(2\left(f_2\right)^2\right)^n$	$2^{2n}\left(f_1 f_2\right)^n$
$\mathbf{E}_{2,3}^2$ or $\mathbf{B}_{2,3}^2$	$\left(2\left(\frac{1}{16}\right)^2\right)^n$	$\left(2\left(f_3\right)^2\right)^n$	$\left(2\left(f_4\right)^2\right)^n$	$2^{2n}\left(f_3 f_4\right)^n$
$\mathbf{E}_1\mathbf{E}_{2,3}$ or $\mathbf{E}_1\mathbf{B}_{2,3}$ or $\mathbf{B}_1\mathbf{E}_{2,3}$ or $\mathbf{B}_1\mathbf{B}_{2,3}$	$\left(\frac{1}{16}\right)^{2n}$	$\left(f_1\right)^n\left(f_3\right)^n$	$\left(f_2\right)^n\left(f_4\right)^n$	$\left(f_2\right)^n\left(f_3\right)^n+\left(f_1\right)^n\left(f_4\right)^n$
$\mathbf{E}_2\mathbf{E}_3$ or $\mathbf{B}_2\mathbf{B}_3$	$\left(\frac{1}{16}\right)^{2n}$	$\left(f_3\right)^{2n}$	$\left(f_4\right)^{2n}$	$2\left(f_3\right)^n\left(f_4\right)^n$
$\mathbf{E}_2\mathbf{B}_2$ or $\mathbf{E}_3\mathbf{B}_3$	$\left(\left(\frac{1}{16}\right)^2\right)^n$	$\left(f_3\right)^{2n}$	$\left(f_4\right)^{2n}$	$2\left(f_3\right)^n\left(f_4\right)^n$
$\mathbf{E}_1\mathbf{B}_1$	$\left(\frac{1}{16}\right)^{2n}$	$\left(f_1\right)^{2n}$	$\left(f_2\right)^{2n}$	$2\left(f_1\right)^n\left(f_2\right)^n$
Functions	$f_1=-\frac{(\ell-2t)(\ell+t)^2}{64t^3}$	$f_2=\frac{(\ell+2t)(\ell-t)^2}{64t^3}$	$f_3=\frac{\ell^3+3\ell t^2+4t^3}{128t^3}$	$f_4=\frac{-\ell^3-3\ell t^2+4t^3}{128t^3}$

Table B.2: $\Delta S_{\mathcal{A}}^{(n)}\left[\mathcal{O}\right]=\frac{1}{1-n}\log\left[\frac{N_1+N_2+N_3}{D_1}\right]$ in the region $0<\ell<t$.

$\mathcal{O}$	D_1	N_1	N_2	P_1	P_2	P_3
$\mathbf{E}_2\mathbf{B}_3$ or $\mathbf{B}_2\mathbf{E}_3$	$\left(2^2\left(\frac{1}{4\cdot 8}\right)\right)$	$(2g_1^2+2g_3^2)^n$	$(22g_2^2+2g_4^2)^n$	$2^{2n}g_2^n g_3^n$	$2^{2n}g_1^n g_4^n$	0

Table B.3: $\Delta S_{\mathcal{A}}^{(n)}\left[\mathcal{O}\right]=-\frac{1}{n-1}\log\left[\frac{N_1+N_2+P_1+P_2+P_3}{D_1}\right]$ in the region $0<\ell<t$.

We have again as the result a sum of functions in the power of n. The time evolution of the Rényi EE growth for the excited state of $\mathbf{E}_1\mathbf{E}_1$ and $\mathbf{E}_2\mathbf{E}_2$ is shown in figure B.2, as well as for $\mathbf{E}_1\mathbf{E}_2$, $\mathbf{E}_2\mathbf{E}_3$ and $\mathbf{E}_1\mathbf{B}_1$ in B.3. In both cases, we see that the time evolution is slower if the excitation includes more operators in x^1 direction.

For $\mathbf{E}_2\mathbf{B}_3$ and $\mathbf{B}_2\mathbf{E}_3$, we have the expression

$$\Delta S_{\mathcal{A}}^{(n)}=-\frac{1}{n-1}\log\left[\frac{N_1+N_2+P_1+P_2+P_3}{D_1}\right], \tag{B.16}$$

where the functions N_i, P_i are listed in the table B.3, using functions g_i defined as

$$\begin{aligned}
g_1&=\frac{(\ell+t)^3}{4\cdot 64t^3},\\
g_2&=\frac{(t-\ell)^3}{4\cdot 64t^3},\\
g_3&=\frac{(\ell+t)\left(l^2-4\ell t+7t^2\right)}{4\cdot 64t^3},\\
g_4&=\frac{(t-\ell)\left(\ell^2+4\ell t+7t^2\right)}{4\cdot 64t^3}.
\end{aligned} \tag{B.17}$$

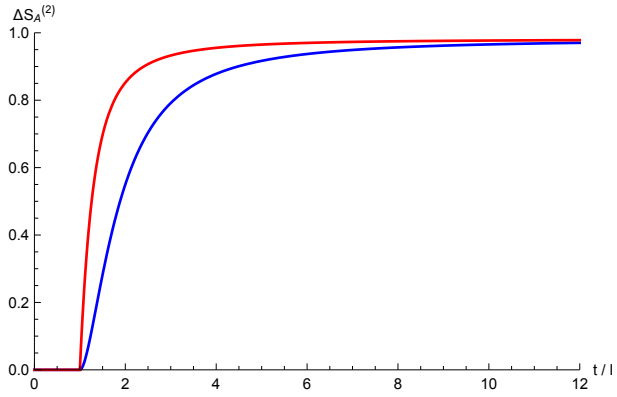

Figure B.2: The time evolution of $\Delta S_{\mathcal{A}}^{(2)}$ for $\mathbf{E}_1\mathbf{E}_1$ and $\mathbf{E}_2\mathbf{E}_2$. The horizontal and vertical axes correspond to time t/ℓ and the excess of $\Delta S_{\mathcal{A}}^{(2)}$, respectively. The lower curve represents the evolution for $\mathbf{E}_1\mathbf{E}_1$, and the upper curve for $\mathbf{E}_2\mathbf{E}_2$. In the limit $t \to \infty$, they are all $\log \frac{8}{3}$.

The time evolution of $\mathbf{E}_1\mathbf{E}_2, \mathbf{E}_2\mathbf{E}_3, \mathbf{E}_1\mathbf{B}_1$ is shown in figure B.3, based on the results listed in the table B.2. We can again see that $\Delta S_{\mathcal{A}}^{(n)}$ is 0 until the time $t = \ell$, and then its value starts to increase.

In the late late time limit $t \to \infty$, $\Delta S_{\mathcal{A}}^{(n)}$ and $\Delta S_{\mathcal{A}}^{(1)}$ differs depending on how the state is excited. For the excitation E_iE_j or B_iB_j, when $i = j$ the value is

$$\Delta S_{\mathcal{A}}^{(n)} = -\frac{1}{1-n} \log \frac{4^n}{2^n + 2}, \tag{B.18}$$

$$\Delta S_{\mathcal{A}}^{(1)} = \frac{3}{2} \log 2 \tag{B.19}$$

and when $i \neq j$, it is

$$\Delta S_{\mathcal{A}}^{(n)} = \Delta S_{\mathcal{A}}^{(1)} = 2 \log 2 \tag{B.20}$$

From this result, we observe again that Rényi EE growth $\Delta S_{\mathcal{A}}^{(n)}$ are invariant under the transformation $\mathbf{E}_i \to -\mathbf{B}_i$ and $\mathbf{B}_i \to \mathbf{E}_i$.

Finally, we evaluate the linear combination of composite operators, including the Lorentz invariant combinations. The results are summarized in table B.4, where we use the same expression in eq. (B.16) with the definition in eq. (B.17). The time evolution of $\mathbf{E}^2$, $F_{\mu\nu}F^{\mu\nu}$ and $\mathbf{B}_2\mathbf{E}_3 - \mathbf{B}_3\mathbf{E}_2$ are displayed in fig B.4. The late time

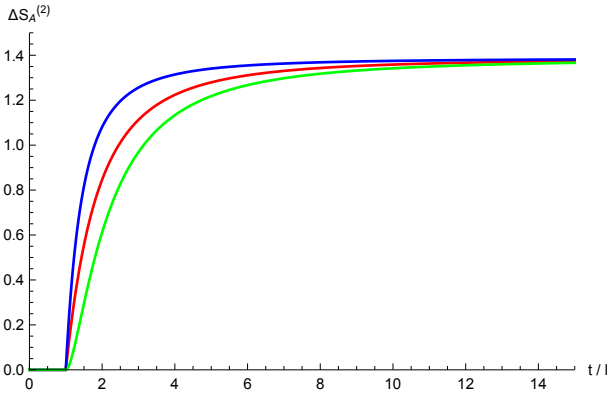

Figure B.3: The time evolution of $\Delta S_{\mathcal{A}}^{(2)}$ for $\mathbf{E}_1\mathbf{E}_2$, $\mathbf{E}_2\mathbf{E}_3$ ($\mathbf{E}_2\mathbf{B}_2$) and $\mathbf{E}_1\mathbf{B}_1$. The horizontal and vertical axes correspond to time t/ℓ and the excess of $\Delta S_{\mathcal{A}}^{(2)}$, respectively. The curve in the middle represents the evolution for $\mathbf{E}_1\mathbf{E}_2$, the upper curve for $\mathbf{E}_2\mathbf{E}_3$ ($\mathbf{E}_2\mathbf{B}_2$) and the lower curve for $\mathbf{E}_1\mathbf{B}_1$, respectively. In the limit $t/\ell \to \infty$, they are all $2\log 2$.

$\mathcal{O}$	D_1	N_1	N_2	P_1	P_2	P_3
$\mathbf{B}^2 or \mathbf{E}^2$	$\left(2\cdot 3\left(\frac{1}{16}\right)^2\right)^n$	$(2f_1^2+2\cdot 2f_3^2)^n$	$(2f_2^2+2\cdot 2f_4^2)^n$	$2^{2n}f_1^n f_2^n$	$2^{2n}f_3^n f_4^n$	$2^{2n}f_3^n f_4^n$
$B_1^2+E_1^2$	$\left(2\cdot 2\left(\frac{1}{16}\right)^2\right)^n$	$(2\cdot 2f_1^2)^n$	$(2\cdot 2f_2^2)^n$	$2^{2n}f_1^n f_2^n$	$2^{2n}f_1^n f_2^n$	0
$F^{\mu\nu}F_{\mu\nu}$ or $\mathbf{B}\cdot\mathbf{E}$	$\left(2\cdot 2\left(\frac{1}{16}\right)^2+2\cdot 4^2\left(\frac{1}{4\cdot 8}\right)^2\right)^n$	$(2\cdot 2f_1^2+2\cdot 4^2 g_1\cdot g_3)^n$	$(2\cdot 2f_2^2+2\cdot 4^2 g_2\cdot g_4)^n$	$2\cdot 2^{2n}(f_1)^n(f_2)^n$	$2\cdot 4^{2n}(g_1)^n(g_2)^n$	$2\cdot 4^{2n}(g_3)^n(g_4)^n$
$B_2E_3-B_3E_2$	$\left(4\cdot 2\left(\frac{1}{4\cdot 8}\right)^2\right)^n$	$(2\cdot 2g_3^2+2\cdot 2g_1^2)^n$	$(2\cdot 2g_4^2+2\cdot 2g_2^2)^n$	$2^{2n}(g_3)^n(g_2)^n$	$2^{2n}(g_1)^n(g_4)^n$	0
Functions	$g_1=\frac{(\ell+t)^3}{4\cdot 64t^3}$	$g_2=\frac{(t-\ell)^3}{4\cdot 64t^3}$	$g_3=\frac{(\ell+t)(\ell^2-4\ell t+7t^2)}{4\cdot 64t^3}$	$g_4=\frac{(t-\ell)(\ell^2+4\ell t+7t^2)}{4\cdot 64t^3}$		

Table B.4: $\Delta S_{\mathcal{A}}^{(n)}[\mathcal{O}]=\frac{1}{1-n}\log\left[\frac{N_1+N_2+P_1+P_2+P_3}{D_1}\right]$ in the region $0<l<t$

value of them varies. For excitations $E_1^2+B_1^2$, the late time value is $\log 4$. For $\mathbf{E}_2\mathbf{B}_3$ or $\mathbf{E}_3\mathbf{B}_2$, the late time value of $\Delta S_{\mathcal{A}}^{(n)}$ is given by

$$\Delta S_{\mathcal{A}}^{(n)}=-\frac{\log(2^{1-6n}(7^n+25^n)}{n-1}. \tag{B.21}$$

When we have the excitations with $\mathbf{B}\cdot\mathbf{E}$ or $F_{\mu\nu}F^{\mu\nu}$,

$$\Delta S_{\mathcal{A}}^{(n)}=\frac{1}{n-1}\log\left(\frac{2^{6n-1}3^n}{16^n+30^n+49^n+1}\right), \tag{B.22}$$

and for the case of $\mathbf{B}_2\mathbf{E}_3-\mathbf{B}_3\mathbf{E}_2$,

$$\Delta S_{\mathcal{A}}^{(n)}=-\frac{\log(2^{1-7n}(2\cdot 7^n+50^n))}{n-1}. \tag{B.23}$$

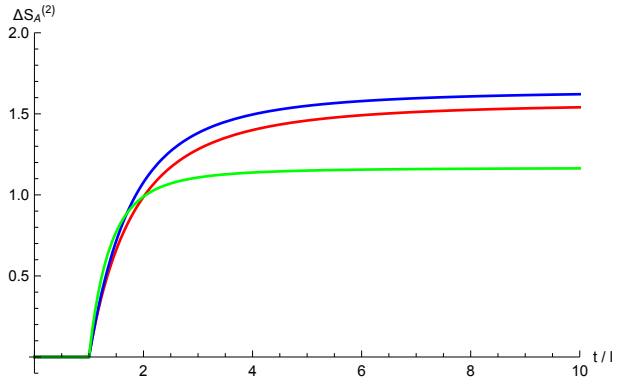

Figure B.4: The time evolution of $\mathbf{E}^2$, $F^{\mu\nu}F_{\mu\nu}$ and $\mathbf{B}_2\mathbf{E}_3 - \mathbf{B}_3\mathbf{E}_2$. The horizontal and vertical axes correspond to time t/ℓ and the excess of $\Delta S_{\mathcal{A}}^{(2)}$ respectively. The curve which is asymptotically in the middle represents the evolution for $\mathbf{E}^2$, the one which is asymptotically on top for $F^{\mu\nu}F_{\mu\nu}$, and the one which is asymptotically lowest for $\mathbf{B}_2\mathbf{E}_3 - \mathbf{B}_3\mathbf{E}_2$, respectively.

We can see from fig B.4, that for each case we have a different late time value. The excitation with $\mathbf{B}_2\mathbf{E}_3 - \mathbf{E}_2\mathbf{B}_3$ has the smallest late time value, but when we look at $\frac{t}{\ell} \sim 1$ the same excitation has the strongest increase of entanglement. Physically, this can be understood since that excitation is the Poynting vector towards the entangling surface.

Bibliography

[1] A. Einstein, B. Podolsky, and N. Rosen, "Can quantum-mechanical description of physical reality be considered complete?," *Phys. Rev.*, vol. 47, pp. 777–780, May 1935.

[2] J. F. Clauser and A. Shimony, "Bell's theorem: Experimental tests and implications," *Rept. Prog. Phys.*, vol. 41, pp. 1881–1927, 1978.

[3] Ken Kawarabayashi, *Quantum Mechanics (in Japanese)*. Iwanami, 2001.

[4] A. Renyi, "On measures of entropy and information," *Proceedings of the Fourth Berkeley Symposium on Mathematics, Statics and Probability*, vol. 1, pp. 547–561, 1961.

[5] R. D. Sorkin, "On the entropy of the vacuum outside a horizon," in *General Relativity and Gravitation*, vol. 1, p. 734, 1983.

[6] L. Bombelli, R. K. Koul, J. Lee, and R. D. Sorkin, "A Quantum Source of Entropy for Black Holes," *Phys. Rev.*, vol. D34, pp. 373–383, 1986.

[7] M. Srednicki, "Entropy and area," *Phys. Rev. Lett.*, vol. 71, pp. 666–669, 1993.

[8] D. N. Kabat, "Black hole entropy and entropy of entanglement," *Nucl. Phys.*, vol. B453, pp. 281–299, 1995.

[9] A. D. Barvinsky and S. N. Solodukhin, "Nonminimal coupling, boundary terms and renormalization of the Einstein-Hilbert action and black hole entropy," *Nucl. Phys.*, vol. B479, pp. 305–318, 1996.

[10] W. Donnelly and A. C. Wall, "Do gauge fields really contribute negatively to black hole entropy?," *Phys. Rev.*, vol. D86, p. 064042, 2012.

[11] S. N. Solodukhin, "Remarks on effective action and entanglement entropy of Maxwell field in generic gauge," *JHEP*, vol. 12, p. 036, 2012.

[12] L. De Nardo, D. V. Fursaev, and G. Miele, "Heat kernel coefficients and spectra of the vector Laplacians on spherical domains with conical singularities," *Class. Quant. Grav.*, vol. 14, pp. 1059–1078, 1997.

[13] D. Iellici and V. Moretti, "Kabat's surface terms in the zeta function approach," in *General relativity and gravitational physics. Proceedings, 12th Italian Conference, Rome, Italy, September 23-27, 1996*, pp. 317–321, 1996.

[14] G. Cognola and P. Lecca, "Electromagnetic fields in Schwarzschild and Reissner-Nordstrom geometry. Quantum corrections to the black hole entropy," *Phys. Rev.*, vol. D57, pp. 1108–1111, 1998.

[15] D. Kabat and D. Sarkar, "Cosmic string interactions induced by gauge and scalar fields," *Phys. Rev.*, vol. D86, p. 084021, 2012.

[16] W. Donnelly and A. C. Wall, "Entanglement entropy of electromagnetic edge modes," *Phys. Rev. Lett.*, vol. 114, no. 11, p. 111603, 2015.

[17] S. Aoki, T. Iritani, M. Nozaki, T. Numasawa, N. Shiba, and H. Tasaki, "On the definition of entanglement entropy in lattice gauge theories," *JHEP*, vol. 06, p. 187, 2015.

[18] M. Nozaki, T. Numasawa, and T. Takayanagi, "Quantum Entanglement of Local Operators in Conformal Field Theories," *Phys. Rev. Lett.*, vol. 112, p. 111602, 2014.

[19] M. Nozaki, "Notes on Quantum Entanglement of Local Operators," *JHEP*, vol. 10, p. 147, 2014.

[20] M. Nozaki, T. Numasawa, and S. Matsuura, "Quantum Entanglement of Fermionic Local Operators," *JHEP*, vol. 02, p. 150, 2016.

[21] M. Nozaki and N. Watamura, "Quantum Entanglement of Locally Excited States in Maxwell Theory," *JHEP*, vol. 12, p. 069, 2016.

[22] M. Nozaki and N. Watamura, "Correspondence between entanglement growth and probability distribution of quasiparticles," *Phys. Rev.*, vol. D96, no. 2, p. 025019, 2017.

[23] P. Caputa, J. Simón, A. Štikonas, and T. Takayanagi, "Quantum Entanglement of Localized Excited States at Finite Temperature," *JHEP*, vol. 01, p. 102, 2015.

[24] P. A. M. Dirac, "Note on Exchange Phenomena in the Thomas Atom," *Proceedings of the Cambridge Philosophical Society*, vol. 26, p. 376, 1930.

[25] P. Caputa, M. Nozaki, and T. Takayanagi, "Entanglement of local operators in large-N conformal field theories," *PTEP*, vol. 2014, p. 093B06, 2014.

[26] S. He, T. Numasawa, T. Takayanagi, and K. Watanabe, "Quantum dimension as entanglement entropy in two dimensional conformal field theories," *Phys. Rev.*, vol. D90, no. 4, p. 041701, 2014.

[27] P. Caputa and A. Veliz-Osorio, "Entanglement constant for conformal families," *Phys. Rev.*, vol. D92, no. 6, p. 065010, 2015.

[28] B. Chen, W.-Z. Guo, S. He, and J.-q. Wu, "Entanglement Entropy for Descendent Local Operators in 2D CFTs," *JHEP*, vol. 10, p. 173, 2015.

[29] H. Casini and M. Huerta, "A c-theorem for the entanglement entropy," *J. Phys.*, vol. A40, pp. 7031–7036, 2007.

[30] H. Casini and M. Huerta, "Universal terms for the entanglement entropy in 2+1 dimensions," *Nucl. Phys.*, vol. B764, pp. 183–201, 2007.

[31] H. Casini, "Mutual information challenges entropy bounds," *Class. Quant. Grav.*, vol. 24, pp. 1293–1302, 2007.